



Deposited via The University of Sheffield.

White Rose Research Online URL for this paper:

<https://eprints.whiterose.ac.uk/id/eprint/207723/>

Version: Published Version

Article:

Aad, G., Abbott, B., Abeling, K. et al. (2023) Pursuit of paired dijet resonances in the Run 2 dataset with ATLAS. *Physical Review D*, 108. 112005. ISSN: 2470-0010

<https://doi.org/10.1103/physrevd.108.112005>

Reuse

This article is distributed under the terms of the Creative Commons Attribution (CC BY) licence. This licence allows you to distribute, remix, tweak, and build upon the work, even commercially, as long as you credit the authors for the original work. More information and the full terms of the licence here:

<https://creativecommons.org/licenses/>

Takedown

If you consider content in White Rose Research Online to be in breach of UK law, please notify us by emailing eprints@whiterose.ac.uk including the URL of the record and the reason for the withdrawal request.

Pursuit of paired dijet resonances in the Run 2 dataset with ATLAS

G. Aad *et al.**
(ATLAS Collaboration)

 (Received 28 July 2023; accepted 1 November 2023; published 13 December 2023)

New particles with large masses that decay into hadronically interacting particles are predicted by many models of physics beyond the Standard Model. A search for a massive resonance that decays into pairs of dijet resonances is performed using 140 fb^{-1} of proton-proton collisions at $\sqrt{s} = 13 \text{ TeV}$ recorded by the ATLAS detector during Run 2 of the Large Hadron Collider. Resonances are searched for in the invariant mass of the tetrajet system, and in the average invariant mass of the pair of dijet systems. A data-driven background estimate is obtained by fitting the tetrajet and dijet invariant mass distributions with a four-parameter dijet function and a search for local excesses from resonant production of dijet pairs is performed. No significant excess of events beyond the Standard Model expectation is observed, and upper limits are set on the production cross sections of new physics scenarios.

DOI: [10.1103/PhysRevD.108.112005](https://doi.org/10.1103/PhysRevD.108.112005)

I. INTRODUCTION

New massive particles that decay into hadronically interacting quarks and gluons are predicted in many scenarios of physics beyond the Standard Model (BSM) accessible at the Large Hadron Collider (LHC), including well-motivated models of particle dark matter [1–8] and models with large extra spatial dimensions [9–15]. Quarks and gluons produced at high energies fragment and hadronize into collimated *jets* of particles [16], observable in particle detectors like ATLAS [17]. The majority of Standard Model (SM) multijet event production occurs via *nonresonant* quantum chromodynamics (QCD) processes, resulting in multijet systems with smoothly falling invariant mass distributions. The large production cross section of multijet processes can make searching for fully hadronic BSM signatures challenging, especially without the presence of other distinguishing features like leptons and/or missing transverse momentum [18]. However, when massive particles decay into pairs of jets (“dijets”) via *s*-channel interactions, the invariant mass spectrum of the dijet system exhibits the signature of the massive particle as a *resonance* around its mass value. While the rate of new particle production may be too low that no resonance is obvious, such models may be detected using data-driven techniques analyzing the smoothly falling invariant mass distribution of the SM background. Searches for dijet resonances have

been a cornerstone of collider physics at the LHC [19–36] and at earlier colliders [37–40].

This paper presents a search for a generic massive resonance Y that decays into two pairs of intermediate resonances X with the same mass, each decaying into two partons and so typically producing a pair of dijet systems. This decay structure is represented schematically in Fig. 1. Examples of exotic physics models that could produce such a final state topology include scalar diquark [41–44] and coloron states [45–48], and additional new particle content such as vectorlike quarks that interact in pairs with the massive diquark or coloron and decay hadronically [49–51]. The analysis is performed on the Run 2 proton-proton (pp) collision data recorded by the ATLAS experiment. Previous searches for signals with this resonance structure have been performed by the ATLAS [52–55] and CMS [56–58]

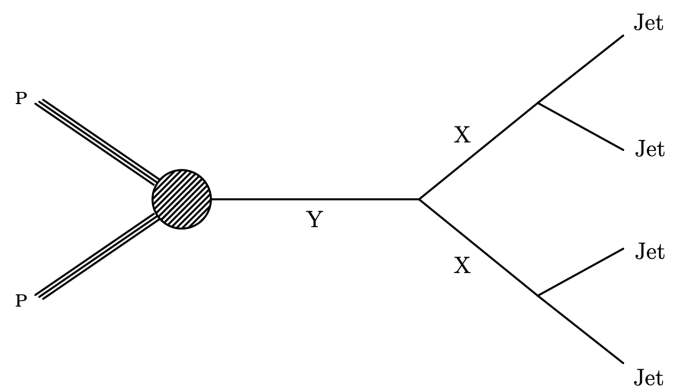


FIG. 1. A schematic representation of the signal topology studied in this analysis: a massive new particle Y decays into two new particles with intermediate mass X , each decaying into a dijet system.

*Full author list given at the end of the article.

Published by the American Physical Society under the terms of the [Creative Commons Attribution 4.0 International license](https://creativecommons.org/licenses/by/4.0/). Further distribution of this work must maintain attribution to the author(s) and the published article's title, journal citation, and DOI. Funded by SCOAP³.

collaborations at the LHC. Most recently, in Ref. [58], the CMS Collaboration studied final states where pairs of dijet resonances are collimated but insufficiently boosted to be reconstructed in a single large-radius jet (e.g., a jet reconstructed with radius parameter $R = 0.8\text{--}1.0$ [59,60]). A small, locally significant excess of events (3.9 standard deviations from two events, corresponding to a 1.6 standard deviation global significance) was observed with tetrajet resonance masses around $m_{4j} \sim 8$ TeV producing dijet resonances with average masses around $m_{2j} \sim 2$ TeV. This prompted an investigation of such final state configurations using ATLAS data.

As there are two resonances with different masses involved in the final state topology (Y and X), both the tetrajet system and the average dijet system invariant masses are separately studied using the BumpHunter algorithm [61–65]. A data-driven background estimate is obtained by fitting these invariant mass distributions with a functional form.

An outline of the remainder of this paper is as follows. Section II provides overviews of the ATLAS detector, the Run 2 pp data sample and the signal and background Monte Carlo (MC) simulations used in this search. This is followed in Sec. III by a description of the analysis methodology including jet reconstruction, event selection, the data-driven background estimation procedure and the systematic uncertainties considered. The main results are presented in Sec. IV, interpreting the observed data in terms of upper limits on the production cross sections of new physics scenarios. Concluding remarks are made in Sec. V.

II. ATLAS, THE RUN 2 DATA, AND SIMULATION

A. The ATLAS detector

The ATLAS detector [17] at the LHC covers nearly the entire solid angle around the collision point.¹ It consists of an inner tracking detector surrounded by a thin superconducting solenoid, electromagnetic and hadron calorimeters, and a muon spectrometer incorporating three large superconducting air-core toroidal magnets.

The inner-detector system is immersed in a 2 T axial magnetic field and provides charged-particle tracking in the range of $|\eta| < 2.5$. The high-granularity silicon pixel detector covers the vertex region and typically provides four measurements per track, the first hit normally being in

the insertable B-layer installed before Run 2 [66,67]. It is followed by the silicon microstrip tracker, which usually provides eight measurements per track. These silicon detectors are complemented by the transition radiation tracker (TRT), which enables radially extended track reconstruction up to $|\eta| = 2.0$. The TRT also provides electron identification information based on the fraction of hits (typically 30 in total) above a higher energy-deposit threshold corresponding to transition radiation.

The calorimeter system covers the pseudorapidity range of $|\eta| < 4.9$. Within the region $|\eta| < 3.2$, electromagnetic calorimetry is provided by barrel and endcap high-granularity lead/liquid-argon (LAr) calorimeters, with an additional thin LAr presampler covering $|\eta| < 1.8$ to correct for energy loss in material upstream of the calorimeters. Hadron calorimetry is provided by the steel/scintillator-tile calorimeter, segmented into three barrel structures with $|\eta| < 1.7$, and two copper/LAr hadron end cap calorimeters. The solid angle coverage is completed with forward copper/LAr and tungsten/LAr calorimeter modules optimized for electromagnetic and hadronic energy measurements respectively.

The muon spectrometer comprises separate trigger and high-precision tracking chambers measuring the deflection of muons in a magnetic field generated by the superconducting air-core toroidal magnets. The field integral of the toroids ranges between 2.0 and 6.0 T m across most of the detector. Three layers of precision chambers, each consisting of layers of monitored drift tubes, cover the region $|\eta| < 2.7$, complemented by cathode-strip chambers in the forward region, where the background is highest. The muon trigger system covers the range of $|\eta| < 2.4$ with resistive-plate chambers in the barrel, and thin-gap chambers in the endcap regions.

Interesting events are selected by the first-level trigger system implemented in custom hardware, followed by selections made by algorithms implemented in software in the high-level trigger [68]. The first-level trigger accepts events from the 40 MHz bunch crossings at a rate below 100 kHz, which the high-level trigger further reduces to record events to disk at about 1 kHz.

An extensive software suite [69] is used in data simulation, in the reconstruction and analysis of real and simulated data, in detector operations, and in the trigger and data acquisition systems of the experiment.

B. The Run 2 data sample

This analysis is performed using data from LHC pp collisions with $\sqrt{s} = 13$ TeV, collected during 2015–2018 with the ATLAS detector. The total integrated luminosity of this data sample is 140 fb^{-1} . The uncertainty in the combined 2015–2018 integrated luminosity is 0.83% [70], obtained using the LUCID-2 detector [71] for the primary luminosity measurements. Due to the high instantaneous luminosity and the large total inelastic pp cross section,

¹ATLAS uses a right-handed coordinate system with its origin at the nominal interaction point (IP) in the center of the detector and the z -axis along the beam pipe. The x -axis points from the IP to the center of the LHC ring, and the y -axis points upward. Cylindrical coordinates (r, ϕ) are used in the transverse plane, ϕ being the azimuthal angle around the z -axis. The pseudorapidity is defined in terms of the polar angle θ as $\eta = -\ln \tan(\theta/2)$. Angular distance is measured in units of $\Delta R \equiv \sqrt{(\Delta y)^2 + (\Delta \phi)^2}$, where $y = (1/2)[(E + p_z)/(E - p_z)]$ is the object's rapidity defined by its energy and longitudinal momentum.

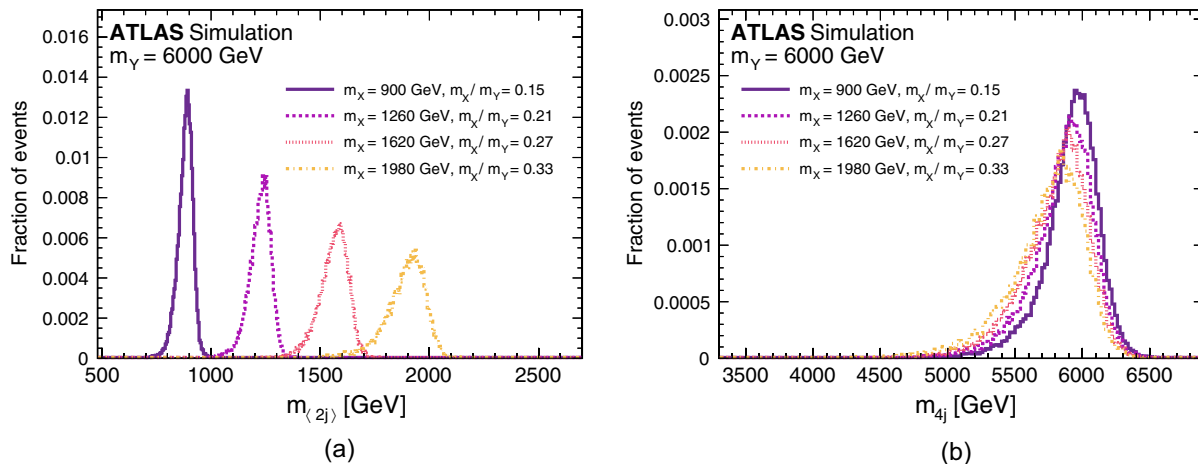


FIG. 2. Examples of (a) $\langle m_{2j} \rangle$ and (b) m_{4j} distributions for $m_Y = 6000$ GeV with $m_X/m_Y = 0.15, 0.21, 0.27,$ and 0.33 .

there are, on average, 33.7 simultaneous collisions (“pileup”) in each bunch crossing. Data are required to satisfy certain quality requirements [72] to be included in the analysis.

During certain data-taking periods, modules of the tile calorimeter were disabled. A study of the impact of vetoing these disabled modules in MC and data was performed, and found to have a negligible impact on the background shape modeling and expected limits.

C. Simulated event samples

Samples of MC simulated signal and background (multi-jet) events are used for optimization, estimation of possible signal contributions, and validation of background estimation strategies.

PYTHIA 8.230 [73,74] was used as the nominal MC generator for both the signal and the background events. Events were simulated using the A14 set of tuned parameters (“tune”) [75], the Lund string hadronization model and the NNPDF2.3LO [76] leading-order (LO) parton distribution function (PDF) set. The PYTHIA parton shower algorithm uses a dipole-style transverse momentum (p_T) ordered evolution, and its renormalization and factorization scales were set to the geometric mean of the squared transverse masses of the outgoing particles. EVTGen [77] was used to model decays of heavy flavor hadrons.

Signal samples were generated with PYTHIA 8.230 using the process $W' \rightarrow WZ$, where the mass of the W' corresponds to the Y mass, and the W/Z masses were both set to be equal to the X mass. The W and Z full widths at half maximum of a relativistic Breit–Wigner were set to 0.1 GeV, so that the width of the resonance is determined by the detector resolution (typically ranging between 1%–4% for both m_{4j} and $\langle m_{2j} \rangle$). These exotic X bosons were forced to decay into quark-antiquark pairs, and decays into top-antitop quark pairs were disabled. Representative m_{4j} and $\langle m_{2j} \rangle$ distributions are shown in Fig. 2 for several

different choices of $\alpha = \langle m_{2j} \rangle / m_{4j}$ (see Sec. III B) with $m_Y = 6000$ GeV. The signal distributions have clear peaks near the generated signal masses.

Background samples of “hard-QCD” multijet processes were simulated using the same PYTHIA settings. These samples were used to optimize aspects of the analysis in early stages, although they are not used for the final background estimate. Additional background multijet samples were simulated with SHERPA 2.2.5 [78] to test the robustness of the background estimation procedure, using the default AHADIC cluster hadronization model [79]. This sample includes LO matrix element calculations for $2 \rightarrow 2$ processes, and used the SHERPA parton shower algorithm based on Catani-Seymour dipole subtraction [80]. It used the CT14NNLO next-to-next-to-leading-order (NNLO) PDF [81] set for matrix element calculations and CT10 for multiparton interactions [82].

Simulated background events were passed through a detailed detector simulation [83] based on Geant4 [84], while simulated signal events were reconstructed with a fast simulation that uses a parametrization of the ATLAS calorimeter response [85]. In both cases, the samples were overlaid with minimum-bias interactions simulated using PYTHIA 8 with the A3 tune [86] and the NNPDF2.3LO PDF set to represent pileup interactions. The distribution of the average number of pileup interactions in simulation is reweighted during data analysis to match that observed in Run 2 data.

Additional details of the MC samples used in this measurement may be found in Ref. [87].

III. METHODOLOGY

A. Particle flow jets

Jets are reconstructed from particle flow objects [88] using the anti- k_r algorithm [89] as implemented in FastJet [90], using a jet radius parameter $R = 0.4$. The ATLAS particle flow algorithm combines measurements

from the ATLAS inner detector and calorimeter systems [91] to improve the jet energy resolution (JER), reduce sensitivity to pileup effects, and improve the jet reconstruction efficiency (especially at low jet p_T) relative to the jet reconstruction based on calorimeter signals alone. Jets are required to have a $p_T > 60$ GeV and a rapidity y satisfying $|y| < 2.4$. The jet energy scale (JES) of particle flow jets is calibrated using a combination of simulation-based and *in situ* corrections [92].

B. Event selection

To be considered for analysis, all detector-level events are required to have at least one primary vertex reconstructed from two or more inner-detector tracks with $p_T > 500$ MeV. Events are required to have at least four jets, from which two dijet pairs are reconstructed. In the selected events, an event selection similar to that of Ref. [58] is applied to allow direct comparisons of the two searches. The two dijet pairs are determined by minimizing the ΔR between the jets, defined as

$$\Delta R = |\Delta R_{AB} - 0.8| + |\Delta R_{CD} - 0.8|,$$

where A, B, C, and D are the ordering of the four highest- p_T jets in the event that minimizes ΔR . The value of 0.8 ensures that the reconstructed pair of dijet systems are collimated, but not so boosted that they will be reconstructed as a large- R jet. Once the two dijet pairs AB and CD are selected, the dijet systems are required to satisfy angular requirements

$$\Delta R_{AB} < 2.0, \quad \Delta R_{CD} < 2.0$$

and

$$\Delta\eta = |\eta_{AB} - \eta_{CD}| < 1.1.$$

In addition, the mass asymmetry between the two dijet pairs is required to satisfy

$$\frac{m_{AB} - m_{CD}}{m_{AB} + m_{CD}} < 0.1.$$

After the event selection procedure is complete, the observables of interest are the invariant mass of the tetrajets system, m_{4j} (a proxy for m_Y), and the average invariant mass of the two dijet systems, $\langle m_{2j} \rangle$ (a proxy for m_X). The ratio of these quantities, $\alpha = \langle m_{2j} \rangle / m_{4j}$, is used to parametrize the kinematic space studied in this search in terms of the Lorentz boost of the X decay products. The correlations between m_{4j} and $\langle m_{2j} \rangle$ are shown in Figs. 3(a) and 3(b) after the event selection for the Run 2 data and for a simulated signal sample with $m_Y = 6$ TeV and $m_X = 2$ TeV, respectively. As shown, requirements on $\langle m_{2j} \rangle$ are correlated with m_{4j} and therefore they can sculpt the background mass

distribution. Figures 3(c)–3(f) illustrate the correlation between m_{4j} , $\langle m_{2j} \rangle$ and α . For the background distribution, α is less correlated with m_{4j} than $\langle m_{2j} \rangle$. The analysis is performed in regions of α rather than $\langle m_{2j} \rangle$, to reduce background sculpting in the tetrajets and average dijet invariant mass spectra due to the selection criteria. Twelve different α regions are used, evenly spaced to cover $0.10 < \alpha < 0.34$. For each α region, separate fits are performed for m_{4j} and $\langle m_{2j} \rangle$.

The combined acceptance times efficiency of all analysis selections is between 12%–45% for signal events as a function of the signal particle masses m_Y and m_X for $2000 \text{ GeV} < m_Y < 10000 \text{ GeV}$, and $500 \text{ GeV} < m_X < 3300 \text{ GeV}$.

Events in data are required to have been selected by one of several single-jet triggers, whose thresholds varied depending on the data-taking period during Run 2. The particular triggers used to select events in a given run period were always the lowest unrescaled triggers recording data during that time. The single jet triggers become fully efficient for different values of m_{4j} and $\langle m_{2j} \rangle$, depending on the α bin that is selected. To use fully efficient triggers while also retaining sensitivity to the widest range of values, different minimum m_{4j} and $\langle m_{2j} \rangle$ thresholds are imposed on the data and simulated signal events used in the interpretation of the search (see Sec. IV). The trigger thresholds were optimized such that they were at least 99.5% efficient for each trigger, and are listed in Table I for the various α regions used in the search. Over 220 000 events in the Run 2 data sample satisfy the analysis selections.

C. Signal templates

The results are interpreted using model-independent and model-dependent strategies. For the model-independent results, the signal templates are modeled as Gaussian distributions, with a mean equal to m_Y and m_X for the m_{4j} and $\langle m_{2j} \rangle$ distributions respectively. Studying a range of template widths is important, as the theoretical width of a signal can vary across possible signal models. In this interpretation, template widths ranging from 5% to 15% for both m_{4j} and $\langle m_{2j} \rangle$ were used. The upper end of the template width is determined from the results of the spurious signal test described in Sec. III D.

For the model-dependent limits, the shape of the m_{4j} and $\langle m_{2j} \rangle$ distributions are parametrized using a crystal ball function [93], which provides a good description of the shape of mass distribution. Signal samples are produced with a limited set of signal masses, and these templates are used as inputs to interpolation between mass points to provide a finer signal grid. The interpolation is done separately for each α region by morphing the parametrized crystal ball fits of the signal shape.

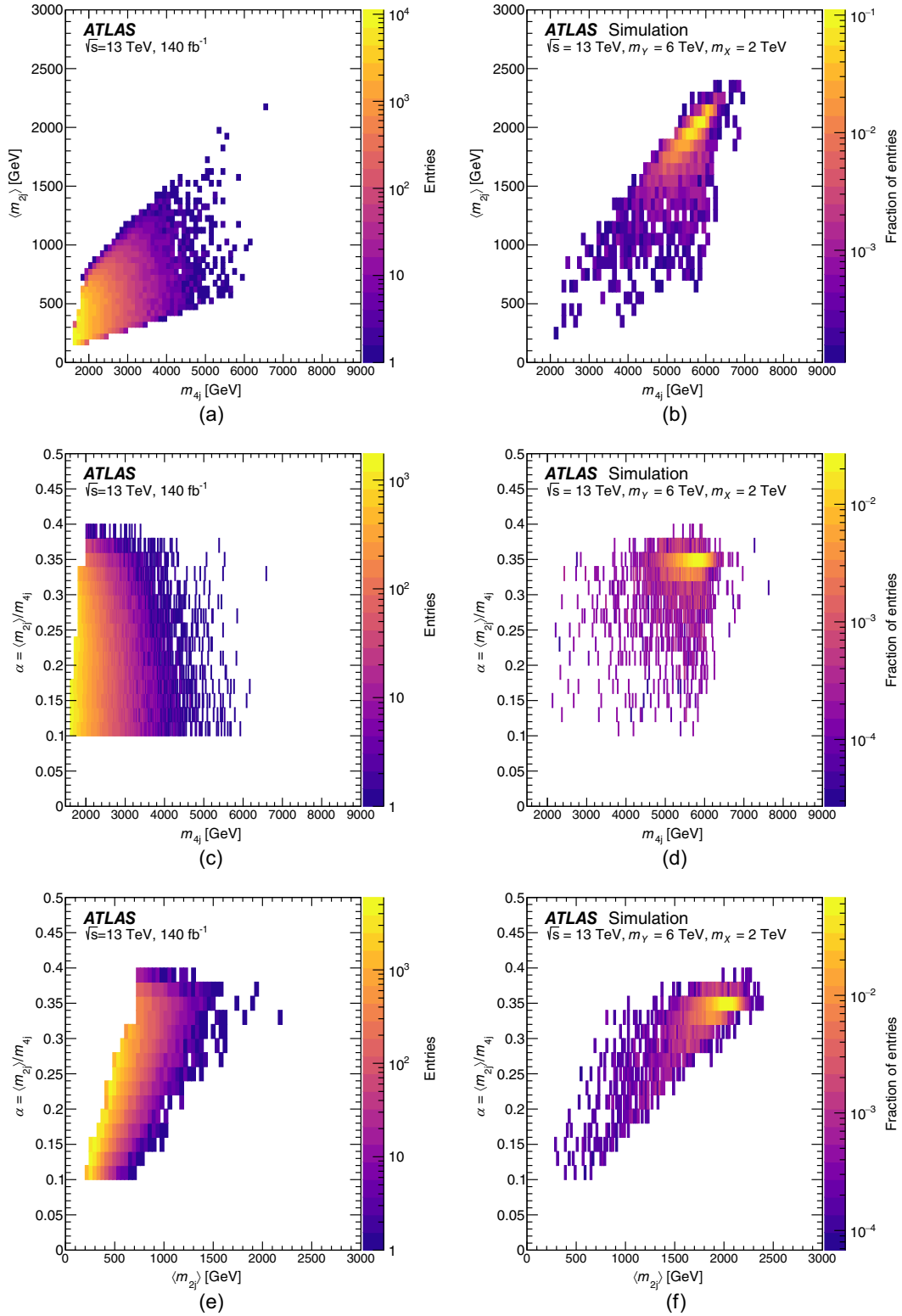


FIG. 3. Two-dimensional histograms of (a),(b) $\langle m_{2j} \rangle$ vs m_{4j} , (c),(d) α vs m_{4j} and (e),(f) α vs $\langle m_{2j} \rangle$. The left column shows the distributions in data, the right column shows the distributions for a simulated signal sample with $m_Y = 6$ TeV and $m_X = 2$ TeV.

TABLE I. Table of selections for the minimum $\langle m_{2j} \rangle$ and m_{4j} values considered when selecting events for a given α bin. These selections are based on a requirement that the single-jet triggers used in the search are at least 99.5% efficient in the selected region.

α bin	Minimum $\langle m_{2j} \rangle$ (GeV)	Minimum m_{4j} (GeV)
$0.10 < \alpha < 0.12$	230	1775
$0.12 < \alpha < 0.14$	250	1775
$0.14 < \alpha < 0.16$	270	1725
$0.16 < \alpha < 0.18$	330	1825
$0.18 < \alpha < 0.20$	370	1875
$0.20 < \alpha < 0.22$	430	1875
$0.22 < \alpha < 0.24$	430	1875
$0.24 < \alpha < 0.26$	490	1875
$0.26 < \alpha < 0.28$	510	1925
$0.28 < \alpha < 0.30$	570	1975
$0.30 < \alpha < 0.32$	630	1975
$0.32 < \alpha < 0.34$	730	2175

D. Background estimation

Nonresonant QCD processes, which constitute the SM background for this search, result in multijet systems with smoothly falling invariant mass distributions. To estimate this background in the search regions, a parametric function is fit to the observed data distributions in 1 GeV bins:

$$f(x) = p_1(1-x)^{p_2}x^{p_3+p_4 \ln(x)+p_5 \ln(x)^2}, \quad x = m/\sqrt{s};$$

where p_1 , p_2 , p_3 , p_4 , and p_5 are the fitted parameters, and m is either m_{4j} or $\langle m_{2j} \rangle$. This function has been successfully used in a wide variety of resonance dijet and multijet searches by the CDF, CMS, and ATLAS experiments [19,22,27,30,32,35,39,58,94]. For the background estimation, a 4-parameter fit is used, where p_5 is set to zero, while the 5-parameter fit is used to produce pseudodata to validate the fit strategy. Three-parameter fit functions were also studied but did not have sufficient flexibility to describe the background.

The background distribution is fit using a binned, maximum-likelihood fit. In background-only fits, the signal strength is set to zero, while in the signal-plus-background fits, the signal strength is left as a free parameter. For the model-dependent interpretation, the signal probability density function is defined as the crystal ball function fit to the simulated signal events. For the model-independent interpretations, the signal is parametrized as a Gaussian distribution, where the signal width is set to be a fixed fraction of the signal peak.

The data-driven background fitting procedure was validated with MC simulation using several cross-checks, including “spurious signal tests” and “signal injection tests.” Tests involving signal-plus-background fits are performed using both templates derived from the simulated signal samples described in Sec. II C, and for model-independent

Gaussian signal shapes, using signal widths of 5%, 10%, and 15% of the signal peak.

The spurious signal test evaluates whether the fitting procedure is biased in a manner that will produce a non-zero extracted signal when fitting a data sample with no true signal. This test is performed for a 4-parameter fit function by performing a signal plus background fit with a Gaussian signal hypothesis of a specified width to 100 pseudodata distributions that are generated from background-only fits to the data distribution with an 5-parameter function, to provide more flexibility to the background distribution than to the fit function. Signal widths for both the X and Y ranging from 5% to 15% of the signal mean are tested, as well as using the signal templates directly. For each pseudodata distribution, the number of extracted signal events, n_S , is determined, and the median value and standard deviation of n_S across all pseudodata distributions are taken to be S_{spur} and σ_{spur} respectively. To satisfy the spurious signal requirements, $S_{\text{spur}}/\sigma_{\text{spur}}$ is required to be less than 0.5. For m_{4j} and $\langle m_{2j} \rangle$, all α regions satisfy this criterion for the signal templates, and for Gaussian signals with widths of 5%, 10%, and 15%.

The signal injection test is performed to ensure that the background fit is able to extract a signal component with the expected signal strength. Simulated signal models with the Gaussian templates with signal widths of 5% to 15% and signal templates are included in the fitted background distribution with a given signal cross section selected to be in the range of $0 - 5\sigma$, where $\sigma = n_S/\sqrt{n_B}$ and the number of signal and background events are determined using a 2σ window around the injected signal peak in each test. For these studies, the extracted signal strength is scaled to be the number of signal events within a 2σ window around the injected signal peak, to match the definition used for the injection. The injected signals in this study were extracted for 100 pseudodata distributions, with the requirement that the median extracted significance is within 0.5σ of the injected significance for fits to both the m_{4j} and $\langle m_{2j} \rangle$ distributions in all analysis α regions. All signal templates and Gaussian signals that passed the spurious signal tests also passed the signal injection tests.

E. Systematic and statistical uncertainties

When interpreting the analysis in terms of candidate signal models, the impact of various experimental and theoretical sources of uncertainty is considered. The uncertainties in the luminosity and parton distribution functions are included as Gaussian constraints on the yield, while the uncertainties in the jet energy scale, jet energy resolution, tune, and theoretical renormalization and factorization scale are included as Gaussian constraints on the shape of the distribution. The uncertainty in the background modeling is implemented as an additional “spurious” signal-like contribution.

1. Luminosity

The uncertainty in the combined 2015–2018 integrated luminosity is 0.83% [70], obtained using the LUCID-2 detector [71] for the primary luminosity measurements. It is treated as a single normalization uncertainty applied as a scale factor to the signal models.

2. Parton distribution functions

The theoretical uncertainty envelope associated with the NNPDF2.3LO set of PDFs is propagated through the analysis, where their impact is primarily on the normalization of the signal events. The change in analysis selection efficiency is recalculated for each provided PDF variation, and the standard deviation of all such variations is taken as a measure of the systematic uncertainty due to the PDFs. This uncertainty is a sub-1% effect for all signal models considered.

3. Jet energy scale and resolution

Systematic uncertainties in the $R = 0.4$ JES and JER are evaluated using a series of *in situ* measurements and simulation-based techniques, documented in Ref. [92]. Improvements have been made to the component of the jet energy scale uncertainty related to the extrapolation of single-hadron response measurements [95,96] and combined test-beam results [97,98] into jets. These uncertainties are reduced by roughly a factor of two compared to those reported in Ref. [92]. Uncertainties due to differences between the gluon-initiated jet energy response of different MC generator setups have also been reduced (“jet flavor response” in Ref. [92]), by performing more granular comparisons of the effect of different parton shower and hadronization models on the jet response using the samples documented in Ref. [87]. Following the improved procedure compared with that documented in Ref. [92], the most significant source of uncertainty in the JES now originates from the absolute *in situ* JES calibration.

4. Variation of initial-state α_S value in the A14 set of tuned parameters

The A14 set of tuned parameters used in the PYTHIA 8 signal simulation includes a pair of “eigentune variations” that can be used to assess the sensitivity of an analysis to the value of the QCD coupling, α_S , in initial-state radiation (ISR) [75]. The value of α_S was varied between 0.115–0.140 from its initial value of 0.127. The impact of this variation is negligible compared with other systematic variations.

5. Theoretical renormalization and factorization scale variations

The QCD renormalization and factorization scales (μ_R, μ_F) used in the parton shower of the PYTHIA 8 signal samples are each varied up and down by a factor of two, via weights provided by the PYTHIA event generator [99].

These variations assess the sensitivity of the analysis to parton shower configurations that contain branchings that may compromise the PYTHIA parton shower’s underlying assumptions. Scale variations for such configurations will result in a large variation for that shower. The theoretical uncertainties resulting from these scale variations in the mean of the signal distribution are typically less than 0.5%, and are smaller than the JES uncertainties.

6. Background modeling

A systematic uncertainty to cover potential modeling biases is accounted for using the spurious signal S_{modeling} . The value of S_{modeling} is determined as the envelope of $|S_{\text{spur}}|$ over m_{4j} and $\langle m_{2j} \rangle$, respectively. This is implemented as an additional signal contribution, such that

$$N_{\text{signal}}(m_{X,Y}) = \sigma_{\text{signal}} \mathcal{L} A \epsilon + S_{\text{modeling}}(m_{X,Y}) \theta_{\text{modeling}},$$

where $N_{\text{signal}}(m_{X,Y})$ is the number of extracted signal events at a given m_X or m_Y , \mathcal{L} , A , and ϵ are the integrated luminosity, acceptance, and efficiency factors respectively and θ_{modeling} is a nuisance parameter associated with the modeling uncertainty. The acceptance is defined as the fraction of simulated events at generator level passing the analysis selection cuts, while the efficiency is the fraction of reconstructed events passing the selection.

IV. RESULTS

A. Search results

Example tetrajet and average dijet invariant mass distributions in data, together with the corresponding fitted background estimates, are shown in Fig. 4 for two representative α regions. The example α regions are selected to show the highest tetrajet invariant mass, and the most significant localized excess observed in data. The data are well-described by the 4-parameter fit function in all α regions, and the global χ^2 p -value ranges from 0.74 to 1.00 for the m_{4j} spectra, and from 0.08 to 1.00 for the $\langle m_{2j} \rangle$ spectra. The BumpHunter [62,63] algorithm, as implemented in pyBumpHunter [64,65], is used to quantify the statistical significance of possible resonant signals that may be present in the m_{4j} and $\langle m_{2j} \rangle$ distributions. This is performed using mass bins where the bin width is determined by the mass resolution of m_{4j} or $\langle m_{2j} \rangle$ as a function of the mass, where the mass resolution is determined using a Gaussian fit to the mass response distribution. The width of the invariant mass window scanned by BumpHunter is varied between two and six resolution bins, and all possible windows of the m_{4j} and $\langle m_{2j} \rangle$ distributions are scanned, in each α region. For each scanned window, BumpHunter evaluates the statistical significance of the observed difference between the data

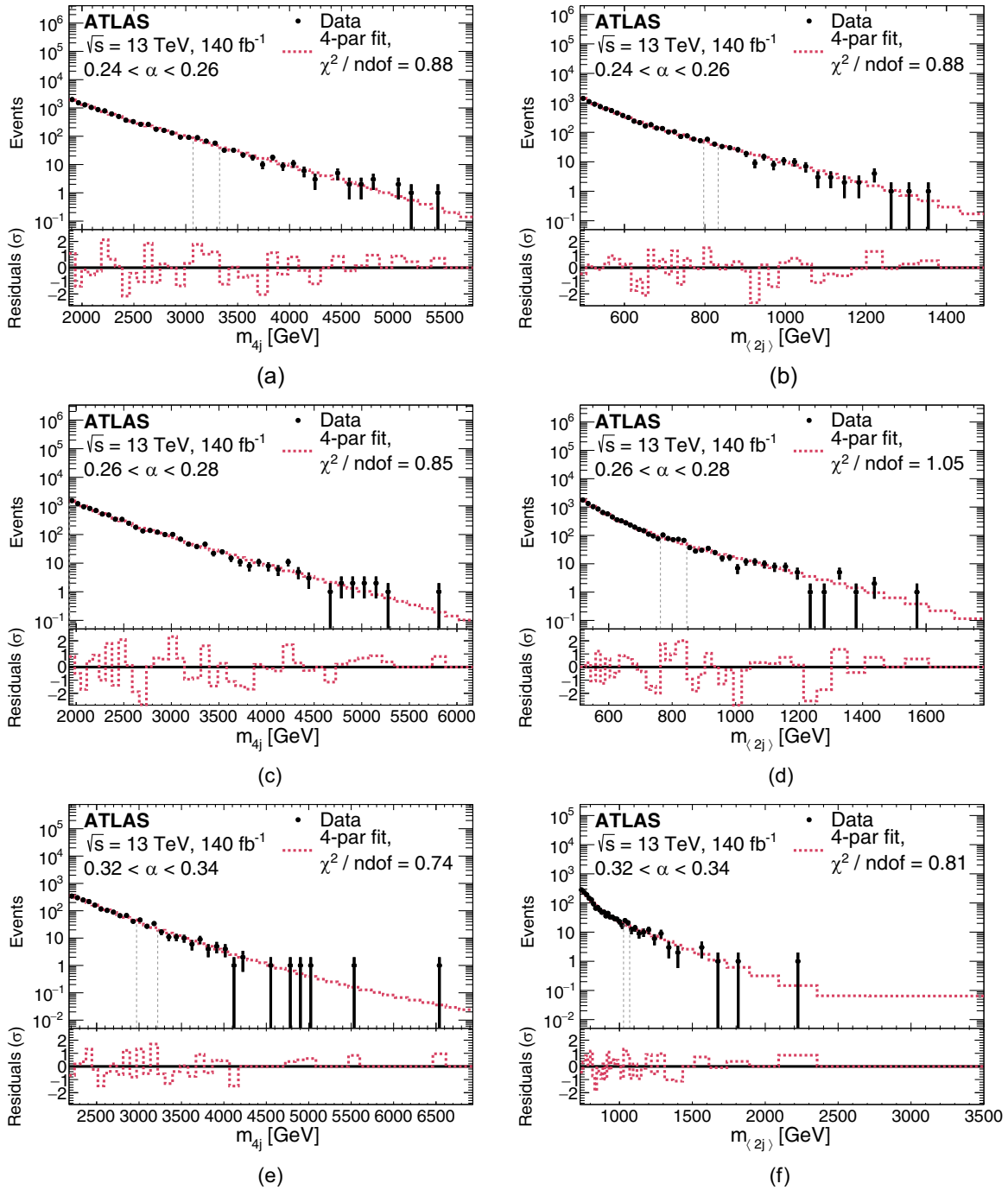


FIG. 4. The (a),(c),(e) tetrajet and (b),(d),(f) average dijet invariant mass distributions in data are shown, along with the fitted background estimates for (a),(b) $0.24 < \alpha < 0.26$, (c),(d) $0.26 < \alpha < 0.28$, and (e),(f) $0.32 < \alpha < 0.34$. The bottom panel of each figure illustrates the fit residuals in terms of standard deviations (σ).

distribution and the background fit. The BumpHunter p -value is defined as the smallest observed probability for the data in a given window to deviate from the background prediction by the observed amount due to a Poissonian fluctuation of the background, using pseudoexperiments generated from the background prediction. The most significant localized

excesses identified by the BumpHunter algorithm are found at 3200 GeV in the α region from $0.24 < \alpha < 0.26$ for the m_{4j} spectra with a global significance of 0.53 standard deviations, and at 800 GeV in the α region from $0.26 < \alpha < 0.28$ for the $\langle m_{2j} \rangle$ spectra with a global significance of 1.98 standard deviations.

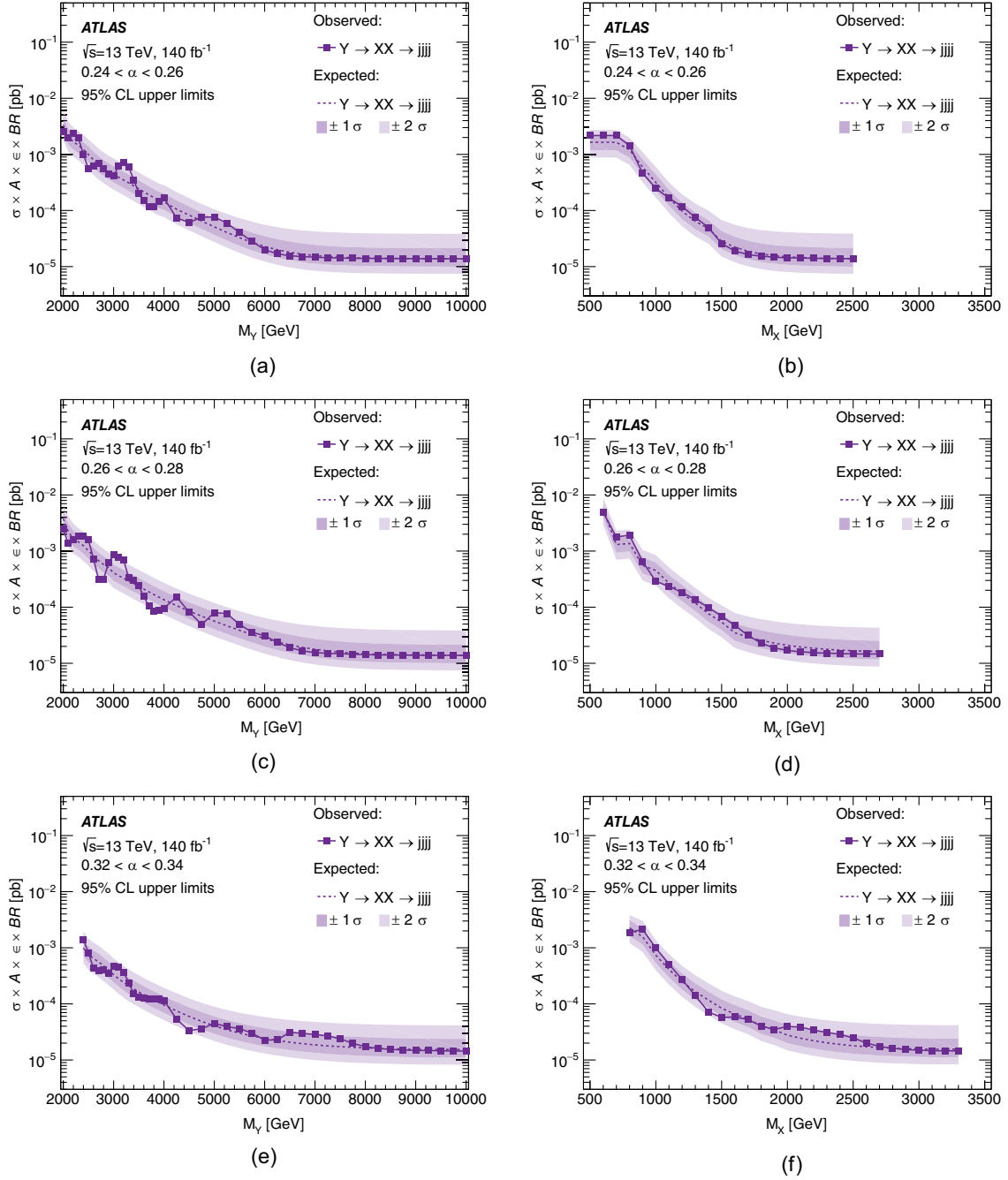


FIG. 5. The expected and observed 95% confidence exclusion limits on the signal cross section times acceptance (A), efficiency (ϵ), and branching ratio (BR) as a function of (a),(c),(e) m_Y and (b),(d),(f) m_X using the signal templates and a 4-parameter fit function for (a),(b) $0.24 < \alpha < 0.26$, (c),(d) $0.26 < \alpha < 0.28$, and (e),(f) $0.32 < \alpha < 0.34$. Observed and expected limits are indicated with markers or a dashed line, respectively. The shaded bands around the expected limit indicates the (darker band) 1σ and (lighter band) 2σ uncertainty range.

B. Cross-section limits

As no signal is observed, limits can be placed on the range of possible production cross sections for the hypothetical Y and X bosons.

The numbers of signal and background events are estimated from maximum-likelihood fits of the

signal-plus-background models to the corresponding m_{4j} and $\langle m_{2j} \rangle$ distributions. Systematic uncertainties described in Sec. III E are included in the fits via nuisance parameters constrained by Gaussian penalty terms. The p -value is determined from a profile-likelihood-ratio test statistic [100]. The local p -value for compatibility with the

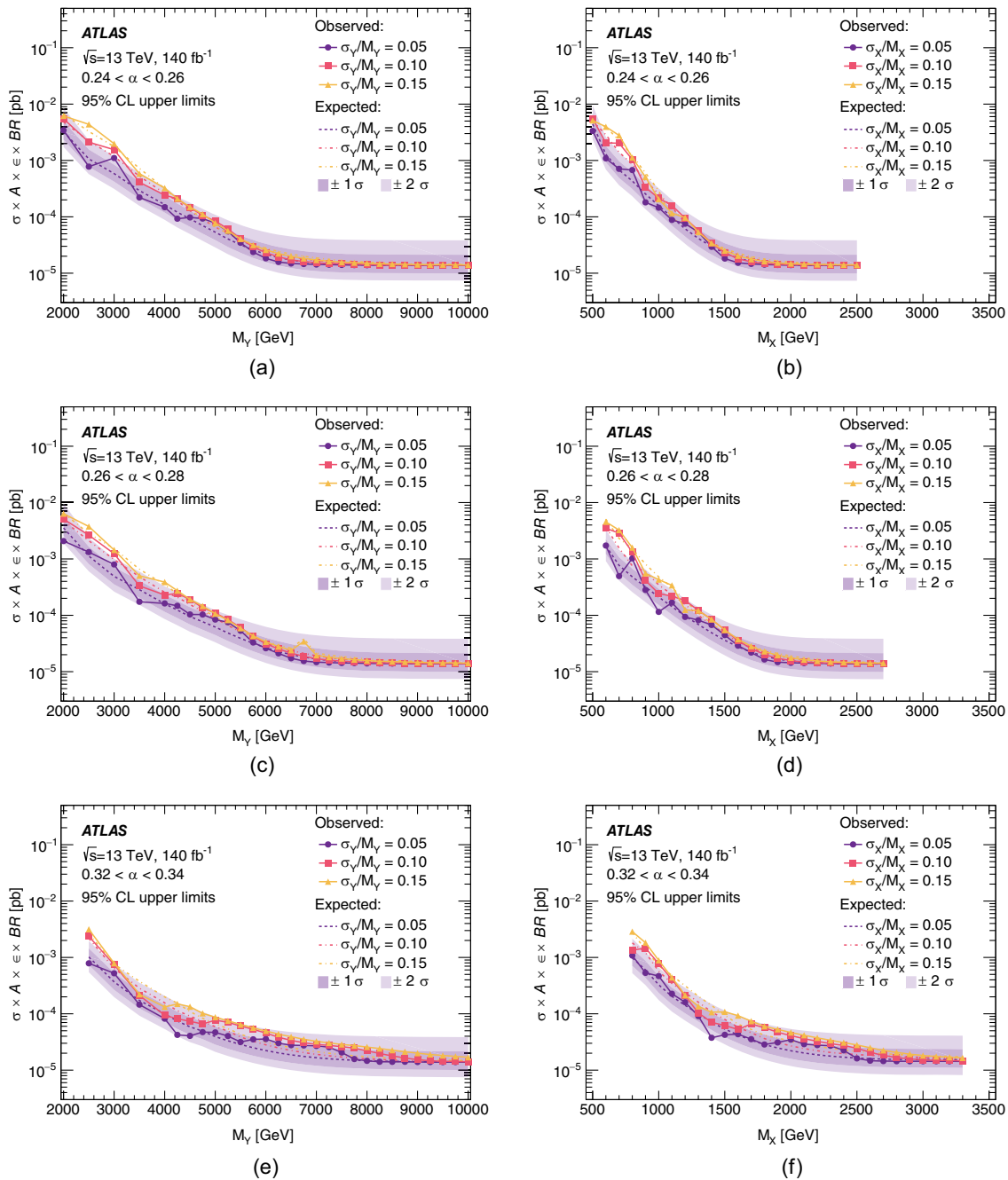


FIG. 6. The expected and observed limits on the signal cross section times acceptance (A), efficiency (ϵ), and branching ratio (BR) as a function of (a),(c),(e) m_Y and (b),(d),(f) m_X for Gaussian signal templates using a 4-parameter fit function for (a),(b) $0.24 < \alpha < 0.26$, (c),(d) $0.26 < \alpha < 0.28$, and (e),(f) $0.32 < \alpha < 0.34$. Observed and expected limits corresponding to different choices of template widths (5%, 10%, and 15%) are indicated as different sets of markers or line styles, respectively. The shaded bands around the expected limit for templates with 5% width indicate the (darker band) 1σ and (lighter band) 2σ uncertainty range.

background-only hypothesis when testing a given signal hypothesis (p_0) is evaluated based on the asymptotic approximation. Global significance values are computed from background-only pseudoexperiments to account for the trial factors due to scanning both the signal mass and the width hypotheses. The expected and observed 95% confidence level (CL) exclusion limits on the product

of the cross section, branching ratio and acceptance are computed using a modified frequentist-approach CL_s [101], in an asymptotic approximation to the test-statistic distribution.

Figure 5 shows the 95% CL upper limits on the allowed cross sections of these particles as a function of their mass, derived using the signal templates used to optimize the

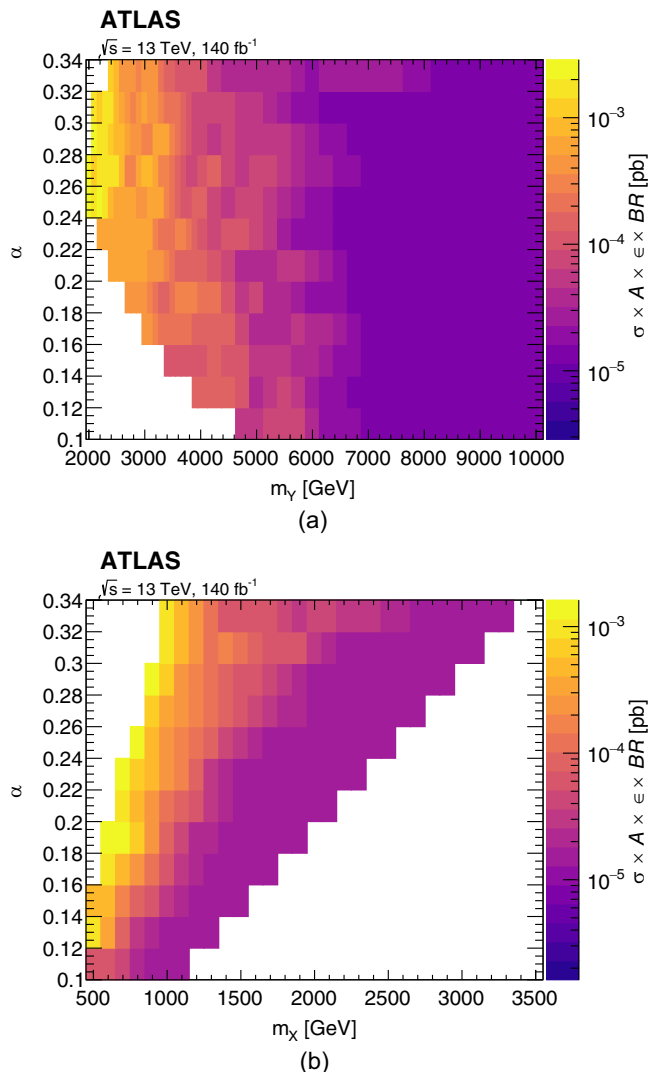


FIG. 7. The observed 95% confidence exclusion limits on the signal cross section times acceptance (A), efficiency (ϵ), and branching ratio (BR) as a function of (a) m_Y , and (b) m_X for signals templates using a 4-parameter fit function.

analysis for two representative α regions. Results are interpolated linearly in the logarithm of the cross section. Similar results are shown in Fig. 6 for the Gaussian signal templates with 5%, 10%, and 15% signal widths. A summary of the limits for all generated signal masses is shown in Fig. 7 for m_Y and m_X as a function of α . Overall, the limits are smooth as a function of the mass and α , and flatten out in the high-mass region where the background estimation predicts significantly less than one event.

The relative contribution of statistical and systematic uncertainties (see Sec. III E) on the final analysis sensitivity was assessed by repeating the limit-setting procedure while including only statistical sources of uncertainty. The analysis sensitivity was not observed to significantly differ during this test.

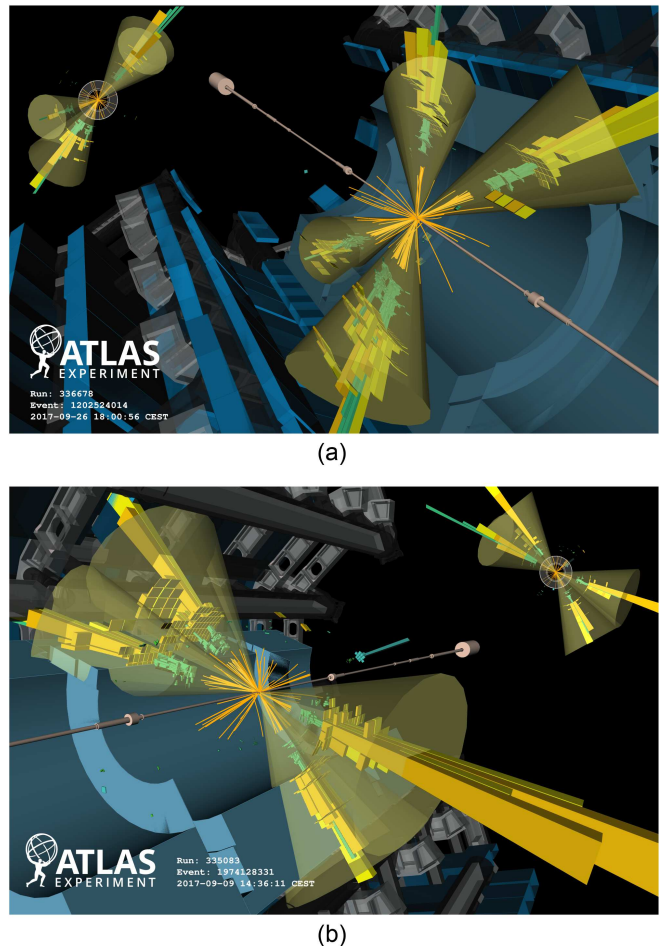


FIG. 8. Event display of multijet events (a) Run 336678, Event 1202524014 and (b) Run 335083, Event 1924128331 from proton-proton collisions recorded by ATLAS with LHC stable beams at a collision energy of 13 TeV. The former event is displayed from a side-view where the beamline runs horizontally across the image, while the latter event is displayed in a transverse view, down the beamline. Event (a) possesses the largest tetrajete invariant mass observed in the search ($m_{4j} = 6.6$ TeV, $\langle m_{2j} \rangle = 2.2$ TeV), and the p_T values of the four selected jets are 2, 1.2, 1.2, and 0.5 TeV. Event (b) is the event with the highest- p_T fourth-jet passing the event selection ($m_{4j} = 5.2$ TeV, $\langle m_{2j} \rangle = 0.90$ TeV), and the p_T values of the four selected jets are 1.6, 1.3, 1.2, and 1.0 TeV. Tracks with momenta greater than 1 GeV are shown as yellow lines, and energy depositions in the Liquid Argon and Tile calorimeters cells are displayed, respectively, as green and yellow boxes.

To better illustrate different types of events passing the event selection, two event displays are shown in Fig. 8. The first shows the event with the highest four-jet mass, with a value of $m_{4j} = 6.6$ TeV and corresponding $\langle m_{2j} \rangle = 2.2$ TeV, while the second shows the event with the highest- p_T fourth jet that is selected ($m_{4j} = 5.2$ TeV, $\langle m_{2j} \rangle = 0.90$ TeV).

V. CONCLUSION

A search for the production of a generic massive resonance Y that decays into two pairs of intermediate resonances X , each decaying into two jets, is performed using 140 fb^{-1} of proton-proton collisions with $\sqrt{s} = 13 \text{ TeV}$ collected with the ATLAS Detector during Run 2 of the LHC. Such a resonant signal in multijet events could be manifested in many models of physics beyond the Standard Model, including in well-motivated models of particle dark matter and models with large extra spatial dimensions.

A data-driven background estimate is obtained by fitting these invariant mass distributions with a functional form. The tetrajets system and average dijet system invariant masses are then studied using the `BumpHunter` algorithm. No significant excess of events beyond the Standard Model expectation is observed. The most significant localized excesses are found at 3200 GeV in the α region from $0.24 < \alpha < 0.26$ for the m_{4j} spectra (global significance of 0.53 standard deviations), and at 800 GeV in the α region from $0.26 < \alpha < 0.28$ for the $\langle m_{2j} \rangle$ spectra (global significance of 1.98 standard deviations). The highest tetrajets invariant mass observed is $m_{4j} = 6.6 \text{ TeV}$, with a corresponding $\langle m_{2j} \rangle$ value of 2.2 TeV . Using the observed data, upper limits are set on the production cross sections of new physics scenarios as a function of the Y and X masses in both the model-dependent and model-independent interpretations.

Data distributions from this search are openly available on the HEPData platform [102] for use in future reinterpretations.

ACKNOWLEDGMENTS

We thank CERN for the very successful operation of the LHC, as well as the support staff from our institutions without whom ATLAS could not be operated efficiently. We acknowledge the support of ANPCyT, Argentina; YerPhI, Armenia; ARC, Australia; BMWFW and FWF, Austria; ANAS, Azerbaijan; CNPq and FAPESP, Brazil; NSERC, NRC and CFI, Canada; CERN; ANID, Chile;

CAS, MOST and NSFC, China; Minciencias, Colombia; MEYS CR, Czech Republic; DNRF and DNSRC, Denmark; IN2P3-CNRS and CEA-DRF/IRFU, France; SRNSFG, Georgia; BMBF, HGF and MPG, Germany; GSRI, Greece; RGC and Hong Kong SAR, China; ISF and Benozziyo Center, Israel; INFN, Italy; MEXT and JSPS, Japan; CNRST, Morocco; NWO, Netherlands; RCN, Norway; MEiN, Poland; FCT, Portugal; MNE/IFA, Romania; MESTD, Serbia; MSSR, Slovakia; ARRS and MIZŠ, Slovenia; DSI/NRF, South Africa; MICINN, Spain; SRC and Wallenberg Foundation, Sweden; SERI, SNSF and Cantons of Bern and Geneva, Switzerland; MOST, Taiwan; TENMAK, Türkiye; STFC, United Kingdom; DOE and NSF, United States of America. In addition, individual groups and members have received support from BCKDF, CANARIE, Compute Canada and CRC, Canada; PRIMUS 21/SCI/017 and UNCE SCI/013, Czech Republic; COST, ERC, ERDF, Horizon 2020, ICSC-NextGenerationEU and Marie Skłodowska-Curie Actions, European Union; Investissements d’Avenir Labex, Investissements d’Avenir IDEX and ANR, France; DFG and AvH Foundation, Germany; Herakleitos, Thales and Aristeia programmes co-financed by EU-ESF and the Greek NSRF, Greece; BSF-NSF and MINERVA, Israel; Norwegian Financial Mechanism 2014–2021, Norway; NCN and NAWA, Poland; La Caixa Banking Foundation, CERCA Programme Generalitat de Catalunya and PROMETEO and GenT Programmes Generalitat Valenciana, Spain; Göran Gustafssons Stiftelse, Sweden; The Royal Society and Leverhulme Trust, United Kingdom. The crucial computing support from all WLCG partners is acknowledged gratefully, in particular from CERN, the ATLAS Tier-1 facilities at TRIUMF (Canada), NDGF (Denmark, Norway, Sweden), CC-IN2P3 (France), KIT/GridKA (Germany), INFN-CNAF (Italy), NL-T1 (Netherlands), PIC (Spain), ASGC (Taiwan), RAL (United Kingdom) and BNL (USA), the Tier-2 facilities worldwide and large non-WLCG resource providers. Major contributors of computing resources are listed in Ref. [103].

-
- [1] G. Hinshaw *et al.*, Nine-year Wilkinson Microwave Anisotropy Probe (WMAP) observations: Cosmological parameter results, *Astrophys. J. Suppl. Ser.* **208**, 19 (2013).
 - [2] Y. Akrami *et al.*, Planck 2018 results. I. Overview and the cosmological legacy of Planck, *Astron. Astrophys.* **641**, A1 (2020).
 - [3] V. Trimble, Existence and nature of dark matter in the universe, *Annu. Rev. Astron. Astrophys.* **25**, 425 (1987).
 - [4] G. Bertone, D. Hooper, and J. Silk, Particle dark matter: Evidence, candidates and constraints, *Phys. Rep.* **405**, 279 (2005).
 - [5] J. L. Feng, Dark matter candidates from particle physics and methods of detection, *Annu. Rev. Astron. Astrophys.* **48**, 495 (2010).
 - [6] M. Roos, Astrophysical and cosmological probes of dark matter, *J. Mod. Phys.* **3**, 1152 (2012).

- [7] S. Arrenberg *et al.*, Dark matter in the coming decade: Complementary paths to discovery and beyond, [arXiv: 1310.8621](#).
- [8] ATLAS Collaboration, Constraints on mediator-based dark matter and scalar dark energy models using $\sqrt{s} = 13$ TeV pp collision data collected by the ATLAS detector, *J. High Energy Phys.* **05** (2019) 142.
- [9] N. Boelaert and T. Akesson, Dijet angular distributions at $\sqrt{s} = 14$ TeV, *Eur. Phys. J. C* **66**, 343 (2010).
- [10] D. M. Gingrich, Quantum black holes with charge, colour, and spin at the LHC, *J. Phys. G* **37**, 105008 (2010).
- [11] X. Calmet, W. Gong, and S. D. H. Hsu, Colorful quantum black holes at the LHC, *Phys. Lett. B* **668**, 20 (2008).
- [12] S. B. Giddings and S. D. Thomas, High energy colliders as black hole factories: The end of short distance physics, *Phys. Rev. D* **65**, 056010 (2002).
- [13] S. Dimopoulos and G. L. Landsberg, Black holes at the Large Hadron Collider, *Phys. Rev. Lett.* **87**, 161602 (2001).
- [14] P. Meade and L. Randall, Black holes and quantum gravity at the LHC, *J. High Energy Phys.* **05** (2008) 003.
- [15] L. A. Anchordoqui, J. L. Feng, H. Goldberg, and A. D. Shapere, Inelastic black hole production and large extra dimensions, *Phys. Lett. B* **594**, 363 (2004).
- [16] G. P. Salam, Towards jetography, *Eur. Phys. J. C* **67**, 637 (2010).
- [17] ATLAS Collaboration, The ATLAS experiment at the CERN Large Hadron Collider, *J. Instrum.* **3**, S08003 (2008).
- [18] ATLAS Collaboration, Performance of missing transverse momentum reconstruction with the ATLAS detector using proton-proton collisions at $\sqrt{s} = 13$ TeV, *Eur. Phys. J. C* **78**, 903 (2018).
- [19] ATLAS Collaboration, Search for new particles in two-jet final states in 7 TeV proton-proton collisions with the ATLAS detector at the LHC, *Phys. Rev. Lett.* **105**, 161801 (2010).
- [20] CMS Collaboration, Search for dijet resonances in 7 TeV pp collisions at CMS, *Phys. Rev. Lett.* **105**, 211801 (2010).
- [21] ATLAS Collaboration, A search for new physics in dijet mass and angular distributions in pp collisions at $\sqrt{s} = 7$ TeV measured with the ATLAS detector, *New J. Phys.* **13**, 053044 (2011).
- [22] CMS Collaboration, Search for resonances in the dijet mass spectrum from 7 TeV pp collisions at CMS, *Phys. Lett. B* **704**, 123 (2011).
- [23] ATLAS Collaboration, ATLAS search for new phenomena in dijet mass and angular distributions using pp collisions at $\sqrt{s} = 7$ TeV, *J. High Energy Phys.* **01** (2013) 029.
- [24] ATLAS Collaboration, Search for new physics in the dijet mass distribution using 1 fb^{-1} of pp collision data at $\sqrt{s} = 7$ TeV collected by the ATLAS detector, *Phys. Lett. B* **708**, 37 (2012).
- [25] CMS Collaboration, Search for narrow resonances and quantum black holes in inclusive and b -tagged dijet mass spectra from pp collisions at $\sqrt{s} = 7$ TeV, *J. High Energy Phys.* **01** (2013) 013.
- [26] CMS Collaboration, Search for narrow resonances using the dijet mass spectrum in pp collisions at $\sqrt{s} = 8$ TeV, *Phys. Rev. D* **87**, 114015 (2013).
- [27] ATLAS Collaboration, Search for new phenomena in the dijet mass distribution using pp collision data at $\sqrt{s} = 8$ TeV with the ATLAS detector, *Phys. Rev. D* **91**, 052007 (2015).
- [28] CMS Collaboration, Search for resonances and quantum black holes using dijet mass spectra in proton-proton collisions at $\sqrt{s} = 8$ TeV, *Phys. Rev. D* **91**, 052009 (2015).
- [29] CMS Collaboration, Search for narrow resonances in dijet final states at $\sqrt{s} = 8$ TeV with the novel CMS technique of data scouting, *Phys. Rev. Lett.* **117**, 031802 (2016).
- [30] ATLAS Collaboration, Search for new phenomena in dijet mass and angular distributions from pp collisions at $\sqrt{s} = 13$ TeV with the ATLAS detector, *Phys. Lett. B* **754**, 302 (2016).
- [31] CMS Collaboration, Search for narrow resonances decaying to dijets in proton-proton collisions at $\sqrt{s} = 13$ TeV, *Phys. Rev. Lett.* **116**, 071801 (2016).
- [32] CMS Collaboration, Search for dijet resonances in proton-proton collisions at $\sqrt{s} = 13$ TeV and constraints on dark matter and other models, *Phys. Lett. B* **769**, 520 (2017).
- [33] ATLAS Collaboration, Search for new phenomena in dijet events using 37 fb^{-1} of pp collision data collected at $\sqrt{s} = 13$ TeV with the ATLAS detector, *Phys. Rev. D* **96**, 052004 (2017).
- [34] CMS Collaboration, Search for narrow and broad dijet resonances in proton-proton collisions at $\sqrt{s} = 13$ TeV and constraints on dark matter mediators and other new particles, *J. High Energy Phys.* **08** (2018) 130.
- [35] ATLAS Collaboration, Search for new resonances in mass distributions of jet pairs using 139 fb^{-1} of pp collisions at $\sqrt{s} = 13$ TeV with the ATLAS detector, *J. High Energy Phys.* **03** (2020) 145.
- [36] CMS Collaboration, Search for high mass dijet resonances with a new background prediction method in proton-proton collisions at $\sqrt{s} = 13$ TeV, *J. High Energy Phys.* **05** (2020) 033.
- [37] UA1 Collaboration, Two-jet mass distributions at the CERN proton-antiproton collider, *Phys. Lett. B* **209**, 127 (1988).
- [38] UA2 Collaboration, A search for new intermediate vector mesons and excited quarks decaying to two jets at the CERN $\bar{p}p$ collider, *Nucl. Phys.* **B400**, 3 (1993).
- [39] CDF Collaboration, Search for new particles decaying into dijets in proton-antiproton collisions at $\sqrt{s} = 1.96$ TeV, *Phys. Rev. D* **79**, 112002 (2009).
- [40] D0 Collaboration, Measurement of dijet angular distributions at $\sqrt{s} = 1.96$ TeV and searches for quark compositeness and extra spatial dimensions, *Phys. Rev. Lett.* **103**, 191803 (2009).
- [41] R. N. Mohapatra, N. Okada, and H.-B. Yu, Diquark Higgs at LHC, *Phys. Rev. D* **77**, 011701 (2008).
- [42] T. Han, I. Lewis, and T. McElmurry, QCD corrections to scalar diquark production at hadron colliders, *J. High Energy Phys.* **01** (2010) 123.

- [43] P. Richardson and D. Winn, Simulation of sextet diquark production, *Eur. Phys. J. C* **72**, 1862 (2012).
- [44] N. Assad, B. Fornal, and B. Grinstein, Baryon number and lepton universality violation in leptoquark and diquark models, *Phys. Lett. B* **777**, 324 (2018).
- [45] R. S. Chivukula, A. G. Cohen, and E. H. Simmons, New strong interactions at the Tevatron?, *Phys. Lett. B* **380**, 92 (1996).
- [46] Y. Bai and B. A. Dobrescu, Heavy octets and Tevatron signals with three or four b jets, *J. High Energy Phys.* **07** (2011) 100.
- [47] R. S. Chivukula, A. Farzinnia, J. Ren, and E. H. Simmons, Constraints on the scalar sector of the renormalizable Coloron model, *Phys. Rev. D* **88**, 075020 (2013); **89**, 059905(E) (2014).
- [48] Y. Bai and B. A. Dobrescu, Collider tests of the renormalizable Coloron model, *J. High Energy Phys.* **04** (2018) 114.
- [49] C. Kilic, T. Okui, and R. Sundrum, Colored resonances at the Tevatron: Phenomenology and discovery potential in multijets, *J. High Energy Phys.* **07** (2008) 038.
- [50] Y. Bai and J. Shelton, Composite octet searches with jet substructure, *J. High Energy Phys.* **07** (2012) 067.
- [51] B. A. Dobrescu, R. M. Harris, and J. Isaacson, Ultraheavy resonances at the LHC: Beyond the QCD background, [arXiv:1810.09429](https://arxiv.org/abs/1810.09429).
- [52] ATLAS Collaboration, Search for pair-produced massive coloured scalars in four-jet final states with the ATLAS detector in proton-proton collisions at $\sqrt{s} = 7$ TeV, *Eur. Phys. J. C* **73**, 2263 (2013).
- [53] ATLAS Collaboration, A search for top squarks with R -parity-violating decays to all-hadronic final states with the ATLAS detector in $\sqrt{s} = 8$ TeV proton-proton collisions, *J. High Energy Phys.* **06** (2016) 067.
- [54] ATLAS Collaboration, A search for pair-produced resonances in four-jet final states at $\sqrt{s} = 13$ TeV with the ATLAS detector, *Eur. Phys. J. C* **78**, 250 (2018).
- [55] ATLAS Collaboration, Dijet resonance search with weak supervision using $\sqrt{s} = 13$ TeV pp collisions in the ATLAS detector, *Phys. Rev. Lett.* **125**, 131801 (2020).
- [56] CMS Collaboration, Search for pair-produced resonances decaying to jet pairs in proton-proton collisions at $\sqrt{s} = 8$ TeV, *Phys. Lett. B* **747**, 98 (2015).
- [57] CMS Collaboration, Search for pair-produced resonances decaying to quark pairs in proton-proton collisions at $\sqrt{s} = 13$ TeV, *Phys. Rev. D* **98**, 112014 (2018).
- [58] CMS Collaboration, Search for resonant and nonresonant production of pairs of dijet resonances in proton-proton collisions at $\sqrt{s} = 13$ TeV, *J. High Energy Phys.* **07** (2023) 161.
- [59] CMS Collaboration, Jet energy scale and resolution in the CMS experiment in pp collisions at 8 TeV, *J. Instrum.* **12**, P02014 (2017).
- [60] ATLAS Collaboration, Optimisation of large-radius jet reconstruction for the ATLAS detector in 13 TeV proton-proton collisions, *Eur. Phys. J. C* **81**, 334 (2020).
- [61] G. Choudalakis, Model independent search for new physics at the Tevatron, Ph.D. thesis, MIT, 2008.
- [62] CDF Collaboration, Global search for new physics with 2.0 fb^{-1} at CDF, *Phys. Rev. D* **79**, 011101 (2009).
- [63] G. Choudalakis, On hypothesis testing, trials factor, hypertests and the BumpHunter, in *Proceedings, PHYSTAT 2011 Workshop on Statistical Issues Related to Discovery Claims in Search Experiments and Unfolding*, CERN, Geneva, Switzerland, 2011 (2011), [arXiv:1101.0390](https://arxiv.org/abs/1101.0390).
- [64] L. Vaslin, S. Calvet, V. Barra, and J. Donini, pyBumpHunter: A model independent bump hunting tool in Python for high energy physics analyses, *SciPost Phys. Codebases* **15** (2023).
- [65] L. Vaslin, J. Donini, J. Eschle, and J. Duarte, pyBumpHunter: v0.4.1, version 0.4.1, <https://github.com/scikit-hep/pyBumpHunter/releases/tag/v0.4.1>, 10.5281/zenodo.7684558 (2023).
- [66] ATLAS Collaboration, ATLAS insertable B-layer, Technical Design Report No. ATLAS-TDR-19; CERN-LHCC-2010-013, 2010, <https://cds.cern.ch/record/1291633>; Addendum, Technical Design Report No. ATLAS-TDR-19-ADD-1; CERN-LHCC-2012-009, 2012, <https://cds.cern.ch/record/1451888>.
- [67] B. Abbott *et al.*, Production and integration of the ATLAS insertable B-layer, *J. Instrum.* **13**, T05008 (2018).
- [68] ATLAS Collaboration, Performance of the ATLAS trigger system in 2015, *Eur. Phys. J. C* **77**, 317 (2017).
- [69] ATLAS Collaboration, The ATLAS Collaboration software and firmware, Report No. ATL-SOFT-PUB-2021-001, 2021.
- [70] ATLAS Collaboration, Luminosity determination in pp collisions at $\sqrt{s} = 13$ TeV using the ATLAS detector at the LHC, [arXiv:2212.09379](https://arxiv.org/abs/2212.09379).
- [71] G. Avoni *et al.*, The new LUCID-2 detector for luminosity measurement and monitoring in ATLAS, *J. Instrum.* **13**, P07017 (2018).
- [72] ATLAS Collaboration, ATLAS data quality operations and performance for 2015–2018 data-taking, *J. Instrum.* **15**, P04003 (2020).
- [73] T. Sjöstrand, S. Ask, J. R. Christiansen, R. Corke, N. Desai, P. Ilten, S. Mrenna, S. Prestel, C. O. Rasmussen, and P. Z. Skands, An introduction to PYTHIA 8.2, *Comput. Phys. Commun.* **191**, 159 (2015).
- [74] T. Sjöstrand, S. Mrenna, and P. Z. Skands, PYTHIA 6.4 physics and manual, *J. High Energy Phys.* **05** (2006) 026.
- [75] ATLAS Collaboration, ATLAS PYTHIA 8 tunes to 7 TeV data, Report No. ATL-PHYS-PUB-2014-021, 2014.
- [76] R. D. Ball *et al.* (NNPDF Collaboration), Parton distributions with LHC data, *Nucl. Phys.* **B867**, 244 (2013).
- [77] D. J. Lange, The gvtGen particle decay simulation package, *Nucl. Instrum. Methods Phys. Res., Sect. A* **462**, 152 (2001).
- [78] T. Gleisberg, S. Höche, F. Krauss, M. Schönherr, S. Schumann, F. Siegert, and J. Winter, Event generation with SHERPA 1.1, *J. High Energy Phys.* **02** (2009) 007.
- [79] B. R. Webber, A QCD model for jet fragmentation including soft gluon interference, *Nucl. Phys.* **B238**, 492 (1984).
- [80] S. Schumann and F. Krauss, A parton shower algorithm based on Catani–Seymour dipole factorisation, *J. High Energy Phys.* **03** (2008) 038.
- [81] S. Dulat, T.-J. Hou, J. Gao, M. Guzzi, J. Huston, P. Nadolsky, J. Pumplin, C. Schmidt, D. Stump, and C.-P. Yuan, New parton distribution functions from a

- global analysis of quantum chromodynamics, *Phys. Rev. D* **93**, 033006 (2016).
- [82] H.-L. Lai, M. Guzzi, J. Huston, Z. Li, P. M. Nadolsky, J. Pumplin, and C.-P. Yuan, New parton distributions for collider physics, *Phys. Rev. D* **82**, 074024 (2010).
- [83] ATLAS Collaboration, The ATLAS simulation infrastructure, *Eur. Phys. J. C* **70**, 823 (2010).
- [84] S. Agostinelli *et al.*, Geant4—A simulation toolkit, *Nucl. Instrum. Methods Phys. Res., Sect. A* **506**, 250 (2003).
- [85] ATLAS Collaboration, The simulation principle and performance of the ATLAS fast calorimeter simulation FastCaloSim, Report No. ATL-PHYS-PUB-2010-013, 2010.
- [86] ATLAS Collaboration, The PYTHIA 8 A3 tune description of ATLAS minimum bias and inelastic measurements incorporating the Donnachie–Landshoff diffractive model, Report No. ATL-PHYS-PUB-2016-017, 2016.
- [87] ATLAS Collaboration, Multijet simulation for 13 TeV ATLAS analyses, Report No. ATL-PHYS-PUB-2019-017, 2019.
- [88] ATLAS Collaboration, Jet reconstruction and performance using particle flow with the ATLAS detector, *Eur. Phys. J. C* **77**, 466 (2017).
- [89] M. Cacciari, G. P. Salam, and G. Soyez, The anti- k_r jet clustering algorithm, *J. High Energy Phys.* **04** (2008) 063.
- [90] M. Cacciari, G. P. Salam, and G. Soyez, FastJet user manual, *Eur. Phys. J. C* **72**, 1896 (2012).
- [91] ATLAS Collaboration, Topological cell clustering in the ATLAS calorimeters and its performance in LHC Run 1, *Eur. Phys. J. C* **77**, 490 (2017).
- [92] ATLAS Collaboration, Jet energy scale and resolution measured in proton-proton collisions at $\sqrt{s} = 13$ TeV with the ATLAS detector, *Eur. Phys. J. C* **81**, 689 (2020).
- [93] M. Oreglia, A study of the reactions $\psi' \rightarrow \gamma\gamma\psi$, Ph.D. thesis, Stanford University, 1980.
- [94] ATLAS Collaboration, Search for new phenomena in multi-body invariant masses in events with at least one isolated lepton and two jets using $\sqrt{s} = 13$ TeV proton-proton collision data collected by the ATLAS detector, *J. High Energy Phys.* **07** (2022) 202.
- [95] ATLAS Collaboration, A measurement of the calorimeter response to single hadrons and determination of the jet energy scale uncertainty using LHC Run-1 pp -collision data with the ATLAS detector, *Eur. Phys. J. C* **77**, 26 (2017).
- [96] ATLAS Collaboration, Measurement of the energy response of the ATLAS calorimeter to charged pions from $W^\pm \rightarrow \tau^\pm (\rightarrow \pi^\pm \nu_\tau) \nu_\tau$ events in Run 2 data, *Eur. Phys. J. C* **82**, 223 (2021).
- [97] P. Adragna *et al.*, Testbeam studies of production modules of the ATLAS tile calorimeter, *Nucl. Instrum. Methods Phys. Res., Sect. A* **606**, 362 (2009).
- [98] B. Dowler *et al.*, Performance of the ATLAS hadronic end-cap calorimeter in beam tests, *Nucl. Instrum. Methods Phys. Res., Sect. A* **482**, 94 (2002).
- [99] S. Mrenna and P. Skands, Automated parton-shower variations in PYTHIA 8, *Phys. Rev. D* **94**, 074005 (2016).
- [100] G. Cowan, K. Cranmer, E. Gross, and O. Vitells, Asymptotic formulae for likelihood-based tests of new physics, *Eur. Phys. J. C* **71**, 1554 (2011); **73**, 2501(E) (2013).
- [101] A. L. Read, Presentation of search results: The CL_s technique, *J. Phys. G* **28**, 2693 (2002).
- [102] Pursuit of paired dijet resonances in the Run 2 dataset with ATLAS, HEPData (collection), 10.17182/hepdata.140530 (2023).
- [103] ATLAS Collaboration, ATLAS computing acknowledgements, Report No. ATL-SOFT-PUB-2023-001, 2023.

G. Aad^{90b}, B. Abbott¹²⁰, K. Abeling⁵⁵, N. J. Abicht⁴⁹, S. H. Abidi²⁹, A. Aboulhorma^{35e}, H. Abramowicz¹⁵¹, H. Abreu¹⁵⁰, Y. Abulaiti¹¹⁷, B. S. Acharya^{69a,69b,b}, C. Adam Bourdarios⁴, L. Adamczyk^{86a}, S. V. Addepalli²⁶, M. J. Addison¹⁰², J. Adelman¹¹⁵, A. Adiguzel^{21c}, T. Adye¹³⁴, A. A. Affolder¹³⁶, Y. Afik³⁶, M. N. Agaras¹³, J. Agarwala^{73a,73b}, A. Aggarwal¹⁰¹, C. Agheorghiesei^{27c}, A. Ahmad³⁶, F. Ahmadov^{38,c}, W. S. Ahmed¹⁰⁴, S. Ahuja⁹⁶, X. Ai^{62a}, G. Aielli^{76a,76b}, A. Aikot¹⁶³, M. Ait Tamlihat^{35e}, B. Aitbenkikh^{35a}, I. Aizenberg¹⁶⁹, M. Akbiyik¹⁰¹, T. P. A. Åkesson⁹⁹, A. V. Akimov³⁷, D. Akiyama¹⁶⁸, N. N. Akolkar²⁴, K. Al Khoury⁴¹, G. L. Alberghi^{23b}, J. Albert¹⁶⁵, P. Albicocco⁵³, G. L. Albouy⁶⁰, S. Alderweireldt⁵², M. Aleksa³⁶, I. N. Aleksandrov³⁸, C. Alexa^{27b}, T. Alexopoulos¹⁰, F. Alfonsi^{23b}, M. Algren⁵⁶, M. Alhroob¹²⁰, B. Ali¹³², H. M. J. Ali⁹², S. Ali¹⁴⁸, S. W. Alibocus⁹³, M. Aliev¹⁴⁵, G. Alimonti^{71a}, W. Alkakh⁵⁵, C. Allaire⁶⁶, B. M. M. Allbrooke¹⁴⁶, J. F. Allen⁵², C. A. Allendes Flores^{137f}, P. P. Allport²⁰, A. Aloisio^{72a,72b}, F. Alonso⁹¹, C. Alpigiani¹³⁸, M. Alvarez Estevez¹⁰⁰, A. Alvarez Fernandez¹⁰¹, M. Alves Cardoso⁵⁶, M. G. Alvigi^{72a,72b}, M. Aly¹⁰², Y. Amaral Coutinho^{83b}, A. Ambler¹⁰⁴, C. Amelung³⁶, M. Amerl¹⁰², C. G. Ames¹⁰⁹, D. Amidei¹⁰⁶, S. P. Amor Dos Santos^{130a}, K. R. Amos¹⁶³, V. Ananiev¹²⁵, C. Anastopoulos¹³⁹, T. Andeen¹¹, J. K. Anders³⁶, S. Y. Andreev^{47a,47b}, A. Andreatta^{71a,71b}, S. Angelidakis⁹, A. Angerami^{41,d}, A. V. Anisenkov³⁷, A. Annovi^{74a}, C. Antel⁵⁶, M. T. Anthony¹³⁹, E. Antipov¹⁴⁵, M. Antonelli⁵³, F. Anulli^{75a}, M. Aoki⁸⁴, T. Aoki¹⁵³, J. A. Aparisi Pozo¹⁶³, M. A. Aparo¹⁴⁶, L. Aperio Bella⁴⁸, C. Appelt¹⁸, A. Apyan²⁶, N. Aranzabal³⁶, S. J. Arbiol Val⁸⁷, C. Arcangeletti⁵³, A. T. H. Arce⁵¹, E. Arena⁹³, J.-F. Arguin¹⁰⁸, S. Argyropoulos⁵⁴, J.-H. Arling⁴⁸, O. Arnaez⁴, H. Arnold¹¹⁴, G. Artoni^{75a,75b}, H. Asada¹¹¹, K. Asai¹¹⁸, S. Asai¹⁵³, N. A. Asbah⁶¹

J. Assahsah^{35d} K. Assamagan²⁹ R. Astalos^{28a} S. Atashi¹⁶⁰ R. J. Atkin^{33a} M. Atkinson¹⁶² H. Atmani^{35f}
 P. A. Atlasiddha¹⁰⁶ K. Augsten¹³² S. Auricchio^{72a,72b} A. D. Auriol²⁰ V. A. Austrup¹⁰² G. Avolio³⁶
 K. Axiotis⁵⁶ G. Azuelos^{108,e} D. Babal^{28b} H. Bachacou¹³⁵ K. Bachas^{152,f} A. Bachiu³⁴ F. Backman^{47a,47b}
 A. Badea⁶¹ P. Bagnaia^{75a,75b} M. Bahmani¹⁸ A. J. Bailey¹⁶³ V. R. Bailey¹⁶² J. T. Baines¹³⁴ L. Baines⁹⁵
 O. K. Baker¹⁷² E. Bakos¹⁵ D. Bakshi Gupta⁸ V. Balakrishnan¹²⁰ R. Balasubramanian¹¹⁴ E. M. Baldin³⁷
 P. Balek^{86a} E. Ballabene^{23b,23a} F. Balli¹³⁵ L. M. Baltes^{63a} W. K. Balunas³² J. Balz¹⁰¹ E. Banas⁸⁷
 M. Bandieramonte¹²⁹ A. Bandyopadhyay²⁴ S. Bansal²⁴ L. Barak¹⁵¹ M. Barakat⁴⁸ E. L. Barberio¹⁰⁵
 D. Barberis^{57b,57a} M. Barbero^{90b} M. Z. Barel¹¹⁴ K. N. Barends^{33a} T. Barillari¹¹⁰ M-S. Barisits³⁶
 T. Barklow¹⁴³ P. Baron¹²² D. A. Baron Moreno¹⁰² A. Baroncelli^{62a} G. Barone²⁹ A. J. Barr¹²⁶ J. D. Barr⁹⁷
 L. Barranco Navarro^{47a,47b} F. Barreiro¹⁰⁰ J. Barreiro Guimarães da Costa^{14a} U. Barron¹⁵¹
 M. G. Barros Teixeira^{130a} S. Barsov³⁷ F. Bartels^{63a} R. Bartoldus¹⁴³ A. E. Barton⁹² P. Bartos^{28a} A. Basan^{101,g}
 M. Baselga⁴⁹ A. Bassalat^{66,h} M. J. Basso^{156a} C. R. Basson¹⁰² R. L. Bates⁵⁹ S. Batlamous^{35e} J. R. Batley³²
 B. Batool¹⁴¹ M. Battaglia¹³⁶ D. Battulga¹⁸ M. Bauce^{75a,75b} M. Bauer³⁶ P. Bauer²⁴ L. T. Bazzano Hurrell³⁰
 J. B. Beacham⁵¹ T. Beau¹²⁷ J. Y. Beaucamp⁹¹ P. H. Beauchemin¹⁵⁸ F. Becherer⁵⁴ P. Bechtler²⁴ H. P. Beck^{19,i}
 K. Becker¹⁶⁷ A. J. Beddall⁸² V. A. Bednyakov³⁸ C. P. Bee¹⁴⁵ L. J. Beemster¹⁵ T. A. Beermann³⁶ M. Begalli^{83d}
 M. Begel²⁹ A. Behera¹⁴⁵ J. K. Behr⁴⁸ J. F. Beirer⁵⁵ F. Beisiegel²⁴ M. Belfkir¹⁵⁹ G. Bella¹⁵¹
 L. Bellagamba^{23b} A. Bellerive³⁴ P. Bellos²⁰ K. Beloborodov³⁷ D. Benckekroun^{35a} F. Bendebba^{35a}
 Y. Benhammou¹⁵¹ M. Benoit²⁹ J. R. Bensinger²⁶ S. Bentvelsen¹¹⁴ L. Beresford⁴⁸ M. Beretta⁵³
 E. Bergeaas Kuutmann¹⁶¹ N. Berger⁴ B. Bergmann¹³² J. Beringer^{17a} G. Bernardi⁵ C. Bernius¹⁴³
 F. U. Bernlochner²⁴ F. Bernon^{36,90b} T. Berry⁹⁶ P. Berta¹³³ A. Berthold⁵⁰ I. A. Bertram⁹² S. Bethke¹¹⁰
 A. Betti^{75a,75b} A. J. Bevan⁹⁵ N. K. Bhalla⁵⁴ M. Bhamjee^{33c} S. Bhatta¹⁴⁵ D. S. Bhattacharya¹⁶⁶ P. Bhattacharai¹⁴³
 V. S. Bhopatkar¹²¹ R. Bi^{29,j} R. M. Bianchi¹²⁹ G. Bianco^{23b,23a} O. Biebel¹⁰⁹ R. Bielski¹²³ M. Biglietti^{77a}
 M. Bindi⁵⁵ A. Bingul^{21b} C. Bini^{75a,75b} A. Biondini⁹³ C. J. Birch-sykes¹⁰² G. A. Bird^{20,134} M. Birman¹⁶⁹
 M. Biros¹³³ S. Biryukov¹⁴⁶ T. Bisanz⁴⁹ E. Bisceglie^{43b,43a} J. P. Biswal¹³⁴ D. Biswas¹⁴¹ A. Bitadze¹⁰²
 K. Björke¹²⁵ I. Bloch⁴⁸ C. Blocker²⁶ A. Blue⁵⁹ U. Blumenschein⁹⁵ J. Blumenthal¹⁰¹ G. J. Bobbink¹¹⁴
 V. S. Bobrovnikov³⁷ M. Boehler⁵⁴ B. Boehm¹⁶⁶ D. Bogavac³⁶ A. G. Bogdanchikov³⁷ C. Bohm^{47a}
 V. Boisvert⁹⁶ P. Bokan⁴⁸ T. Bold^{86a} M. Bomben⁵ M. Bona⁹⁵ M. Boonekamp¹³⁵ C. D. Booth⁹⁶
 A. G. Borbély^{59,k} I. S. Bordulev³⁷ H. M. Borecka-Bielska¹⁰⁸ G. Borissov⁹² D. Bortoletto¹²⁶ D. Boscherini^{23b}
 M. Bosman¹³ J. D. Bossio Sola³⁶ K. Bouaouda^{35a} N. Bouchhar¹⁶³ J. Boudreau¹²⁹ E. V. Bouhova-Thacker⁹²
 D. Boumediene⁴⁰ R. Bouquet¹⁶⁵ A. Boveia¹¹⁹ J. Boyd³⁶ D. Boye²⁹ I. R. Boyko³⁸ J. Bracinik²⁰
 N. Brahimi^{62d} G. Brandt¹⁷¹ O. Brandt³² F. Braren⁴⁸ B. Brau¹⁰³ J. E. Brau¹²³ R. Brenner¹⁶⁹ L. Brenner¹¹⁴
 R. Brenner¹⁶¹ S. Bressler¹⁶⁹ D. Britton⁵⁹ D. Britzger¹¹⁰ I. Brock²⁴ G. Brooijmans⁴¹ W. K. Brooks^{137f}
 E. Brost²⁹ L. M. Brown^{165,l} L. E. Bruce⁶¹ T. L. Bruckler¹²⁶ P. A. Bruckman de Renstrom⁸⁷ B. Brüers⁴⁸
 A. Bruni^{23b} G. Bruni^{23b} M. Bruschi^{23b} N. Bruscinò^{75a,75b} T. Buanes¹⁶ Q. Buat¹³⁸ D. Buchin¹¹⁰
 A. G. Buckley⁵⁹ O. Bulekov³⁷ B. A. Bullard¹⁴³ S. Burdin⁹³ C. D. Burgard⁴⁹ A. M. Burger⁴⁰ B. Burghgrave⁸
 O. Burlayenko⁵⁴ J. T. P. Burr³² C. D. Burton¹¹ J. C. Burzynski¹⁴² E. L. Busch⁴¹ V. Büscher¹⁰¹ P. J. Bussey⁵⁹
 J. M. Butler²⁵ C. M. Buttar⁵⁹ J. M. Butterworth⁹⁷ W. Buttinger¹³⁴ C. J. Buxo Vazquez¹⁰⁷ A. R. Buzykaev³⁷
 S. Cabrera Urbán¹⁶³ L. Cadamuro⁶⁶ D. Caforio⁵⁸ H. Cai¹²⁹ Y. Cai^{14a,14e} Y. Cai^{14c} V. M. M. Cairo³⁶
 O. Cakir^{3a} N. Calace³⁶ P. Calafiura^{17a} G. Calderini¹²⁷ P. Calfayan⁶⁸ G. Callea⁵⁹ L. P. Caloba^{83b} D. Calvet⁴⁰
 S. Calvet⁴⁰ T. P. Calvet^{90b} M. Calvetti^{74a,74b} R. Camacho Toro¹²⁷ S. Camarda³⁶ D. Camarero Muñoz²⁶
 P. Camarri^{76a,76b} M. T. Camerlingo^{72a,72b} D. Cameron^{36,m} C. Camincher¹⁶⁵ M. Campanelli⁹⁷ A. Camplani⁴²
 V. Canale^{72a,72b} A. Canesse¹⁰⁴ J. Cantero¹⁶³ Y. Cao¹⁶² F. Capocasa²⁶ M. Capua^{43b,43a} A. Carbone^{71a,71b}
 R. Cardarelli^{76a} J. C. J. Cardenas⁸ F. Cardillo¹⁶³ G. Carducci^{43b,43a} T. Carli³⁶ G. Carlino^{72a} J. I. Carlotto¹³
 B. T. Carlson^{129,n} E. M. Carlson^{165,156a} L. Carminati^{71a,71b} A. Carnelli¹³⁵ M. Carnesale^{75a,75b} S. Caron¹¹³
 E. Carquin^{137f} S. Carrá^{71a,71b} G. Carratta^{23b,23a} F. Carrio Argos^{33g} J. W. S. Carter¹⁵⁵ T. M. Carter⁵²
 M. P. Casado^{13,o} M. Caspar⁴⁸ F. L. Castillo⁴ L. Castillo Garcia¹³ V. Castillo Gimenez¹⁶³ N. F. Castro^{130a,130e}
 A. Catinaccio³⁶ J. R. Catmore¹²⁵ V. Cavaliere²⁹ N. Cavalli^{23b,23a} V. Cavasinni^{74a,74b} Y. C. Cekmecelioglu⁴⁸
 E. Celebi^{21a} F. Celli¹²⁶ M. S. Centonze^{70a,70b} V. Cepaitis⁵⁶ K. Cerny¹²² A. S. Cerqueira^{83a} A. Cerri¹⁴⁶
 L. Cerrito^{76a,76b} F. Cerutti^{17a} B. Cervato¹⁴¹ A. Cervelli^{23b} G. Cesarini⁵³ S. A. Cetin⁸² Z. Chadi^{35a}

D. Chakraborty¹¹⁵ J. Chan¹⁷⁰ W. Y. Chan¹⁵³ J. D. Chapman³² E. Chapon¹³⁵ B. Chargeishvili^{149b}
 D. G. Charlton²⁰ T. P. Charman⁹⁵ M. Chatterjee¹⁹ C. Chauhan¹³³ S. Chekanov⁶ S. V. Chekulaev^{156a}
 G. A. Chelkov^{38,p} A. Chen¹⁰⁶ B. Chen¹⁵¹ B. Chen¹⁶⁵ H. Chen^{14c} H. Chen²⁹ J. Chen^{62c} J. Chen¹⁴²
 M. Chen¹²⁶ S. Chen¹⁵³ S. J. Chen^{14c} X. Chen^{62c,135} X. Chen^{14b,q} Y. Chen^{62a} C. L. Cheng¹⁷⁰
 H. C. Cheng^{64a} S. Cheong¹⁴³ A. Cheplakov³⁸ E. Cheremushkina⁴⁸ E. Cherepanova¹¹⁴
 R. Cherkaoui El Moursli^{35e} E. Cheu⁷ K. Cheung⁶⁵ L. Chevalier¹³⁵ V. Chiarella⁵³ G. Chiarelli^{74a}
 N. Chiedde^{90b} G. Chiodini^{70a} A. S. Chisholm²⁰ A. Chitan^{27b} M. Chitishvili¹⁶³ M. V. Chizhov³⁸ K. Choi¹¹
 A. R. Chomont^{75a,75b} Y. Chou¹⁰³ E. Y. S. Chow¹¹³ T. Chowdhury^{33g} K. L. Chu¹⁶⁹ M. C. Chu^{64a} X. Chu^{14a,14e}
 J. Chudoba¹³¹ J. J. Chwastowski⁸⁷ D. Cieri¹¹⁰ K. M. Ciesla^{86a} V. Cindro⁹⁴ A. Ciocio^{17a} F. Cirotto^{72a,72b}
 Z. H. Citron^{169,r} M. Citterio^{71a} D. A. Ciubotaru^{27b} B. M. Ciungu¹⁵⁵ A. Clark⁵⁶ P. J. Clark⁵² C. Clarry¹⁵⁵
 J. M. Clavijo Columbie⁴⁸ S. E. Clawson⁴⁸ C. Clement^{47a,47b} J. Clercx⁴⁸ L. Clissa^{23b,23a} Y. Coadou^{90b}
 M. Cobal^{69a,69c} A. Coccaro^{57b} R. F. Coelho Barrue^{130a} R. Coelho Lopes De Sa¹⁰³ S. Coelli^{71a} H. Cohen¹⁵¹
 A. E. C. Coimbra^{71a,71b} B. Cole⁴¹ J. Collot⁶⁰ P. Conde Muiño^{130a,130g} M. P. Connell^{33c} S. H. Connell^{33c}
 I. A. Connelly⁵⁹ E. I. Conroy¹²⁶ F. Conventi^{72a,s} H. G. Cooke²⁰ A. M. Cooper-Sarkar¹²⁶
 A. Cordeiro Oudot Choi¹²⁷ L. D. Corpe⁴⁰ M. Corradi^{75a,75b} F. Corriveau^{104,t} A. Cortes-Gonzalez¹⁸
 M. J. Costa¹⁶³ F. Costanza⁴ D. Costanzo¹³⁹ B. M. Cote¹¹⁹ G. Cowan⁹⁶ K. Cranmer¹⁷⁰ D. Cremonini^{23b,23a}
 S. Crépe-Renaudin⁶⁰ F. Crescioli¹²⁷ M. Cristinziani¹⁴¹ M. Cristoforetti^{78a,78b} V. Croft¹¹⁴ J. E. Crosby¹²¹
 G. Crossetti^{43b,43a} A. Cueto¹⁰⁰ T. Cuhadar Donszelmann¹⁶⁰ H. Cui^{14a,14e} Z. Cui⁷ W. R. Cunningham⁵⁹
 F. Curcio^{43b,43a} P. Czodrowski³⁶ M. M. Czurylo^{63b} M. J. Da Cunha Sargedas De Sousa^{57b,57a}
 J. V. Da Fonseca Pinto^{83b} C. Da Via¹⁰² W. Dabrowski^{86a} T. Dado⁴⁹ S. Dahbi^{33g} T. Dai¹⁰⁶ D. Dal Santo¹⁹
 C. Dallapiccola¹⁰³ M. Dam⁴² G. D'amen²⁹ V. D'Amico¹⁰⁹ J. Damp¹⁰¹ J. R. Dandoy¹²⁸ M. F. Daneri³⁰
 M. Danninger¹⁴² V. Dao³⁶ G. Darbo^{57b} S. Darmora⁶ S. J. Das^{29j} S. D'Auria^{71a,71b} C. David^{156b}
 T. Davidek¹³³ B. Davis-Purcell³⁴ I. Dawson⁹⁵ H. A. Day-hall¹³² K. De⁸ R. De Asmundis^{72a} N. De Biase⁴⁸
 S. De Castro^{23b,23a} N. De Groot¹¹³ P. de Jong¹¹⁴ H. De la Torre¹¹⁵ A. De Maria^{14c} A. De Salvo^{75a}
 U. De Sanctis^{76a,76b} A. De Santo¹⁴⁶ J. B. De Vivie De Regie⁶⁰ D. V. Dedovich³⁸ J. Degens¹¹⁴ A. M. Deiana⁴⁴
 F. Del Corso^{23b,23a} J. Del Peso¹⁰⁰ F. Del Rio^{63a} F. Deliot¹³⁵ C. M. Delitzsch⁴⁹ M. Della Pietra^{72a,72b}
 D. Della Volpe⁵⁶ A. Dell'Acqua³⁶ L. Dell'Asta^{71a,71b} M. Delmastro⁴ P. A. Delsart⁶⁰ S. Demers¹⁷²
 M. Demichev³⁸ S. P. Denisov³⁷ L. D'Eramo⁴⁰ D. Derendarz⁸⁷ F. Derue¹²⁷ P. Dervan⁹³ K. Desch²⁴
 C. Deutsch²⁴ F. A. Di Bello^{57b,57a} A. Di Ciaccio^{76a,76b} L. Di Ciaccio⁴ A. Di Domenico^{75a,75b}
 C. Di Donato^{72a,72b} A. Di Girolamo³⁶ G. Di Gregorio³⁶ A. Di Luca^{78a,78b} B. Di Micco^{77a,77b} R. Di Nardo^{77a,77b}
 C. Diaconu^{90b} M. Diamantopoulou³⁴ F. A. Dias¹¹⁴ T. Dias Do Vale¹⁴² M. A. Diaz^{137a,137b} F. G. Diaz Capriles²⁴
 M. Didenko¹⁶³ E. B. Diehl¹⁰⁶ L. Diehl⁵⁴ S. Díez Cornell⁴⁸ C. Diez Pardos¹⁴¹ C. Dimitriadi^{161,24,161}
 A. Dimitrievska^{17a} J. Dingfelder²⁴ I-M. Dinu^{27b} S. J. Dittmeier^{63b} F. Dittus³⁶ F. Djama^{90b} T. Djobava^{149b}
 J. I. Djuvsland¹⁶ C. Doglioni^{102,99} A. Dohnalova^{28a} J. Dolejsi¹³³ Z. Dolezal¹³³ K. M. Dona³⁹
 M. Donadelli^{83c} B. Dong¹⁰⁷ J. Donini⁴⁰ A. D'Onofrio^{77a,77b} M. D'Onofrio⁹³ J. Dopke¹³⁴ A. Doria^{72a}
 N. Dos Santos Fernandes^{130a} P. Dougan¹⁰² M. T. Dova⁹¹ A. T. Doyle⁵⁹ M. A. Draguet¹²⁶ E. Dreyer¹⁶⁹
 I. Drivas-koulouris¹⁰ M. Drnevich¹¹⁷ A. S. Drobac¹⁵⁸ M. Drozdova⁵⁶ D. Du^{62a} T. A. du Pree¹¹⁴ F. Dubinin³⁷
 M. Dubovsky^{28a} E. Duchovni¹⁶⁹ G. Duckeck¹⁰⁹ O. A. Ducu^{27b} D. Duda⁵² A. Dudarev³⁶ E. R. Duden²⁶
 M. D'uffizi¹⁰² L. Duflost⁶⁶ M. Dührssen³⁶ C. Dülse¹⁷¹ A. E. Dumitriu^{27b} M. Dunford^{63a} S. Dungs⁴⁹
 K. Dunne^{47a,47b} A. Duperrin^{90b} H. Duran Yildiz^{3a} M. Düren⁵⁸ A. Durglishvili^{149b} B. L. Dwyer¹¹⁵
 G. I. Dyckes^{17a} M. Dyndal^{86a} B. S. Dziedzic⁸⁷ Z. O. Earnshaw¹⁴⁶ G. H. Eberwein¹²⁶ B. Eckerova^{28a}
 S. Eggebrecht⁵⁵ E. Egidio Purcino De Souza¹²⁷ L. F. Ehrke⁵⁶ G. Eigen¹⁶ K. Einsweiler^{17a} T. Ekelof¹⁶¹
 P. A. Ekman⁹⁹ S. El Farkh^{35b} Y. El Ghazali^{35b} H. El Jarrari^{35e,148} A. El Moussaouy^{108,u} V. Ellajosyula¹⁶¹
 M. Ellert¹⁶¹ F. Ellinghaus¹⁷¹ N. Ellis³⁶ J. Elmsheuser²⁹ M. Elsing³⁶ D. Emeliyanov¹³⁴ Y. Enari¹⁵³
 I. Ene^{17a} S. Epari¹³ J. Erdmann⁴⁹ P. A. Erland⁸⁷ M. Errenst¹⁷¹ M. Escalier⁶⁶ C. Escobar¹⁶³ E. Etzion¹⁵¹
 G. Evans^{130a} H. Evans⁶⁸ L. S. Evans⁹⁶ M. O. Evans¹⁴⁶ A. Ezhilov³⁷ S. Ezzarqtouni^{35a} F. Fabbri⁵⁹
 L. Fabbri^{23b,23a} G. Facini⁹⁷ V. Fadeyev¹³⁶ R. M. Fakhrutdinov³⁷ S. Falciano^{75a} L. F. Falda Ulhoa Coelho³⁶
 P. J. Falke²⁴ J. Faltova¹³³ C. Fan¹⁶² Y. Fan^{14a} Y. Fang^{14a,14e} M. Fanti^{71a,71b} M. Faraj^{69a,69b} Z. Farazpay⁹⁸
 A. Farbin⁸ A. Farilla^{77a} T. Farooque¹⁰⁷ S. M. Farrington⁵² F. Fassi^{35e} D. Fassouliotis⁹

M. Faucci Giannelli^{76a,76b} W. J. Fawcett³² L. Fayard⁶⁶ P. Federic¹³³ P. Federicova¹³¹ O. L. Fedin^{37,p}
 G. Fedotov³⁷ M. Feickert¹⁷⁰ L. Felgioni^{90b} D. E. Fellers¹²³ C. Feng^{62b} M. Feng^{14b} Z. Feng¹¹⁴
 M. J. Fenton¹⁶⁰ A. B. Fenyuk³⁷ L. Ferencz⁴⁸ R. A. M. Ferguson⁹² S. I. Fernandez Luengo^{137f}
 P. Fernandez Martinez¹³ M. J. V. Fernoux^{90b} J. Ferrando⁴⁸ A. Ferrari¹⁶¹ P. Ferrari^{114,113} R. Ferrari^{73a}
 D. Ferrere⁵⁶ C. Ferretti¹⁰⁶ F. Fiedler¹⁰¹ P. Fiedler¹³² A. Filipčič⁹⁴ E. K. Filmer¹ F. Filthaut¹¹³
 M. C. N. Fiolhais^{130a,130c,v} L. Fiorini¹⁶³ W. C. Fisher¹⁰⁷ T. Fitschen¹⁰² P. M. Fitzhugh¹³⁵ I. Fleck¹⁴¹
 P. Fleischmann¹⁰⁶ T. Flick¹⁷¹ M. Flores^{33d,w} L. R. Flores Castillo^{64a} L. Flores Sanz De Acedo³⁶
 F. M. Follega^{78a,78b} N. Fomin¹⁶ J. H. Foo¹⁵⁵ B. C. Forland⁶⁸ A. Formica¹³⁵ A. C. Forti¹⁰² E. Fortin³⁶
 A. W. Fortman⁶¹ M. G. Foti^{17a} L. Fountas^{9,x} D. Fournier⁶⁶ H. Fox⁹² P. Francavilla^{74a,74b} S. Francescato⁶¹
 S. Franchellucci⁵⁶ M. Franchini^{23b,23a} S. Franchino^{63a} D. Francis³⁶ L. Franco¹¹³ V. Franco Lima³⁶
 L. Franconi⁴⁸ M. Franklin⁶¹ G. Frattari²⁶ A. C. Freegard⁹⁵ W. S. Freund^{83b} Y. Y. Frid¹⁵¹ J. Friend⁵⁹
 N. Fritzsche⁵⁰ A. Froch⁵⁴ D. Froidevaux³⁶ J. A. Frost¹²⁶ Y. Fu^{62a} M. Fujimoto^{118,y}
 E. Fullana Torregrosa^{163,a} K. Y. Fung^{64a} E. Furtado De Simas Filho^{83b} M. Furukawa¹⁵³ J. Fuster¹⁶³
 A. Gabrielli^{23b,23a} A. Gabrielli¹⁵⁵ P. Gadow³⁶ G. Gagliardi^{57b,57a} L. G. Gagnon^{17a} E. J. Gallas¹²⁶
 B. J. Gallop¹³⁴ K. K. Gan¹¹⁹ S. Ganguly¹⁵³ Y. Gao⁵² F. M. Garay Walls^{137a,137b} B. Garcia^{29,j} C. García¹⁶³
 A. Garcia Alonso¹¹⁴ A. G. Garcia Caffaro¹⁷² J. E. García Navarro¹⁶³ M. Garcia-Sciveres^{17a} G. L. Gardner¹²⁸
 R. W. Gardner³⁹ N. Garelli¹⁵⁸ D. Garg⁸⁰ R. B. Garg^{143,z} J. M. Gargan⁵² C. A. Garner¹⁵⁵ C. M. Garvey^{33a}
 P. Gaspar^{83b} V. K. Gassmann¹⁵⁸ G. Gaudio^{73a} V. Gautam¹³ P. Gauzzi^{75a,75b} I. L. Gavrilenko³⁷ A. Gavrilyuk³⁷
 C. Gay¹⁶⁴ G. Gaycken⁴⁸ E. N. Gazis¹⁰ A. A. Geanta^{27b} C. M. Gee¹³⁶ C. Gemme^{57b} M. H. Genest⁶⁰
 S. Gentile^{75a,75b} A. D. Gentry¹¹² S. George⁹⁶ W. F. George²⁰ T. Gerialis⁴⁶ P. Gessinger-Befurt³⁶
 M. E. Geyik¹⁷¹ M. Ghani¹⁶⁷ M. Ghneimat¹⁴¹ K. Ghorbanian⁹⁵ A. Ghosal¹⁴¹ A. Ghosh¹⁶⁰ A. Ghosh⁷
 B. Giacobbe^{23b} S. Giagu^{75a,75b} T. Giani¹¹⁴ P. Giannetti^{74a} A. Giannini^{62a} S. M. Gibson⁹⁶ M. Gignac¹³⁶
 D. T. Gil^{86b} A. K. Gilbert^{86a} B. J. Gilbert⁴¹ D. Gillberg³⁴ G. Gilles¹¹⁴ N. E. K. Gillwald⁴⁸ L. Ginabat¹²⁷
 D. M. Gingrich^{2,e} M. P. Giordani^{69a,69c} P. F. Giraud¹³⁵ G. Giugliarelli^{69a,69c} D. Giugni^{71a} F. Giuli³⁶
 I. Gkialas^{9,x} L. K. Gladilin³⁷ C. Glasman¹⁰⁰ G. R. Gledhill¹²³ G. Glemža⁴⁸ M. Glisic¹²³ I. Gnesi^{43b,aa}
 Y. Go^{29,j} M. Goblirsch-Kolb³⁶ B. Gocke⁴⁹ D. Godin¹⁰⁸ B. Gokturk^{21a} S. Goldfarb¹⁰⁵ T. Golling⁵⁶
 M. G. D. Gololo^{33g} D. Golubkov³⁷ J. P. Gombas¹⁰⁷ A. Gomes^{130a,130b} G. Gomes Da Silva¹⁴¹
 A. J. Gomez Delegido¹⁶³ R. Gonçalves^{130a,130c} G. Gonella¹²³ L. Gonella²⁰ A. Gongadze^{149c} F. Gonnella²⁰
 J. L. Gonski⁴¹ R. Y. González Andana⁵² S. González de la Hoz¹⁶³ S. Gonzalez Fernandez¹³
 R. Gonzalez Lopez⁹³ C. Gonzalez Renteria^{17a} M. V. Gonzalez Rodrigues⁴⁸ R. Gonzalez Suarez¹⁶¹
 S. Gonzalez-Sevilla⁵⁶ G. R. Gonzalvo Rodriguez¹⁶³ L. Goossens³⁶ B. Gorini³⁶ E. Gorini^{70a,70b} A. Gorišek⁹⁴
 T. C. Gosart¹²⁸ A. T. Goshaw⁵¹ M. I. Gostkin³⁸ S. Goswami¹²¹ C. A. Gottardo³⁶ S. A. Gotz¹⁰⁹
 M. Gouighri^{35b} V. Goumarre⁴⁸ A. G. Goussiou¹³⁸ N. Govender^{33c} I. Grabowska-Bold^{86a} K. Graham³⁴
 E. Gramstad¹²⁵ S. Grancagnolo^{70a,70b} M. Grandi¹⁴⁶ C. M. Grant^{1,135} P. M. Gravila^{27f} F. G. Gravili^{70a,70b}
 H. M. Gray^{17a} M. Greco^{70a,70b} C. Greife²⁴ I. M. Gregor⁴⁸ P. Grenier¹⁴³ S. G. Grewe¹¹⁰ C. Grieco¹³
 A. A. Grillo¹³⁶ K. Grimm³¹ S. Grinstein^{13,bb} J.-F. Grivaz⁶⁶ E. Gross¹⁶⁹ J. Grosse-Knetter⁵⁵ C. Grud¹⁰⁶
 J. C. Grundy¹²⁶ L. Guan¹⁰⁶ W. Guan²⁹ C. Gubbels¹⁶⁴ J. G. R. Guerrero Rojas¹⁶³ G. Guerrieri^{69a,69c}
 F. Guescini¹¹⁰ D. Guest¹⁸ R. Gugel¹⁰¹ J. A. M. Guhit¹⁰⁶ A. Guida¹⁸ T. Guillemin⁴ E. Guilloton^{167,134}
 S. Guindon³⁶ F. Guo^{14a,14e} J. Guo^{62c} L. Guo⁴⁸ Y. Guo¹⁰⁶ R. Gupta⁴⁸ S. Gurbuz²⁴ S. S. Gurdasani⁵⁴
 G. Gustavino³⁶ M. Guth⁵⁶ P. Gutierrez¹²⁰ L. F. Gutierrez Zagazeta¹²⁸ M. Gutsche⁵⁰ C. Gutschow⁹⁷
 C. Gwenlan¹²⁶ C. B. Gwilliam⁹³ E. S. Haaland¹²⁵ A. Haas¹¹⁷ M. Habedank⁴⁸ C. Haber^{17a} H. K. Hadavand⁸
 A. Hadeef¹⁰¹ S. Hadzic¹¹⁰ A. I. Hagan⁹² J. J. Hahn¹⁴¹ E. H. Haines⁹⁷ M. Haleem¹⁶⁶ J. Haley¹²¹ J. J. Hall¹³⁹
 G. D. Hallowell^{90b} L. Halser¹⁹ K. Hamano¹⁶⁵ M. Hamer²⁴ G. N. Hamity⁵² E. J. Hampshire⁹⁶ J. Han^{62b}
 K. Han^{62a} L. Han^{14c} L. Han^{62a} S. Han^{17a} Y. F. Han¹⁵⁵ K. Hanagaki⁸⁴ M. Hance¹³⁶ D. A. Hangal^{41,d}
 H. Hanif¹⁴² M. D. Hank¹²⁸ R. Hankache¹⁰² J. B. Hansen⁴² J. D. Hansen⁴² P. H. Hansen⁴² K. Hara¹⁵⁷
 D. Harada⁵⁶ T. Harenberg¹⁷¹ S. Harkusha³⁷ M. L. Harris¹⁰³ Y. T. Harris¹²⁶ J. Harrison¹³ N. M. Harrison¹¹⁹
 P. F. Harrison¹⁶⁷ N. M. Hartman¹¹⁰ N. M. Hartmann¹⁰⁹ Y. Hasegawa¹⁴⁰ R. Hauser¹⁰⁷ C. M. Hawkes²⁰
 R. J. Hawkins³⁶ Y. Hayashi¹⁵³ S. Hayashida¹¹¹ D. Hayden¹⁰⁷ C. Hayes¹⁰⁶ R. L. Hayes¹¹⁴ C. P. Hays¹²⁶
 J. M. Hays⁹⁵ H. S. Hayward⁹³ F. He^{62a} M. He^{14a,14e} Y. He¹⁵⁴ Y. He⁴⁸ N. B. Heatley⁹⁵ V. Hedberg⁹⁹

A. L. Heggelund¹²⁵ N. D. Hehir⁹⁵ C. Heidegger⁵⁴ K. K. Heidegger⁵⁴ W. D. Heidorn⁸¹ J. Heilman³⁴
 S. Heim⁴⁸ T. Heim^{17a} J. G. Heinlein¹²⁸ J. J. Heinrich¹²³ L. Heinrich^{110,cc} J. Hejbal¹³¹ L. Helary⁴⁸
 A. Held¹⁷⁰ S. Hellesund¹⁶ C. M. Helling¹⁶⁴ S. Hellman^{47a,47b} R. C. W. Henderson⁹² L. Henkelmann³²
 A. M. Henriques Correia³⁶ H. Herde⁹⁹ Y. Hernández Jiménez¹⁴⁵ L. M. Herrmann²⁴ T. Herrmann⁵⁰ G. Herten⁵⁴
 R. Hertenberger¹⁰⁹ L. Hervas³⁶ M. E. Hespington¹⁰¹ N. P. Hessey^{156a} H. Hibi⁸⁵ E. Hill¹⁵⁵ S. J. Hillier²⁰
 J. R. Hinds¹⁰⁷ F. Hinterkeuser²⁴ M. Hirose¹²⁴ S. Hirose¹⁵⁷ D. Hirschbuehl¹⁷¹ T. G. Hitchings¹⁰² B. Hiti⁹⁴
 J. Hobbs¹⁴⁵ R. Hobincu^{27e} N. Hod¹⁶⁹ M. C. Hodgkinson¹³⁹ B. H. Hodgkinson³² A. Hoecker³⁶ J. Hofer⁴⁸
 T. Holm²⁴ M. Holzbock¹¹⁰ L. B. A. H. Hommels³² B. P. Honan¹⁰² J. Hong^{62c} T. M. Hong¹²⁹
 B. H. Hooberman¹⁶² W. H. Hopkins⁶ Y. Horii¹¹¹ S. Hou¹⁴⁸ A. S. Howard⁹⁴ J. Howarth⁵⁹ J. Hoya⁶
 M. Hrabovsky¹²² A. Hrynevich⁴⁸ T. Hryn'ova⁴ P. J. Hsu⁶⁵ S.-C. Hsu¹³⁸ Q. Hu^{62a} Y. F. Hu^{14a,14e}
 S. Huang^{64b} X. Huang^{14c} X. Huang^{14a,14e} Y. Huang^{139,dd} Y. Huang^{14a} Z. Huang¹⁰² Z. Hubacek¹³²
 M. Huebner²⁴ F. Huegging²⁴ T. B. Huffman¹²⁶ C. A. Hugli⁴⁸ M. Huhtinen³⁶ S. K. Huiberts¹⁶ R. Hulsken¹⁰⁴
 N. Huseynov¹² J. Huston¹⁰⁷ J. Huth⁶¹ R. Hyneman¹⁴³ G. Iacobucci⁵⁶ G. Iakovidis²⁹ I. Ibragimov¹⁴¹
 L. Iconomidou-Fayard⁶⁶ P. Iengo^{72a,72b} R. Iguchi¹⁵³ T. Iizawa^{126,ee} Y. Ikegami⁸⁴ N. Ilic¹⁵⁵ H. Imam^{35a}
 M. Ince Lezki⁵⁶ T. Ingebretsen Carlson^{47a,47b} G. Introzzi^{73a,73b} M. Iodice^{77a} V. Ippolito^{75a,75b} R. K. Irwin⁹³
 M. Ishino¹⁵³ W. Islam¹⁷⁰ C. Issever^{18,48} S. Istin^{21a,ff} H. Ito¹⁶⁸ J. M. Iturbe Ponce^{64a} R. Iuppa^{78a,78b}
 A. Ivina¹⁶⁹ J. M. Izen⁴⁵ V. Izzo^{72a} P. Jacka^{131,132} P. Jackson¹ R. M. Jacobs⁴⁸ B. P. Jaeger¹⁴²
 C. S. Jagfeld¹⁰⁹ G. Jain^{156a} P. Jain⁵⁴ K. Jakobs⁵⁴ T. Jakoubek¹⁶⁹ J. Jamieson⁵⁹ K. W. Janas^{86a}
 M. Javurkova¹⁰³ F. Jeanneau¹³⁵ L. Jeanty¹²³ J. Jejelava^{149a,gg} P. Jenni^{54,hh} C. E. Jessiman³⁴ S. Jézéquel⁴
 C. Jia^{62b} J. Jia¹⁴⁵ X. Jia⁶¹ X. Jia^{14a,14e} Z. Jia^{14c} S. Jiggins⁴⁸ J. Jimenez Pena¹³ S. Jin^{14c} A. Jinaru^{27b}
 O. Jinnouchi¹⁵⁴ P. Johansson¹³⁹ K. A. Johns⁷ J. W. Johnson¹³⁶ D. M. Jones³² E. Jones⁴⁸ P. Jones³²
 R. W. L. Jones⁹² T. J. Jones⁹³ H. L. Joos^{55,36} R. Joshi¹¹⁹ J. Jovicevic¹⁵ X. Ju^{17a} J. J. Junggeburth^{103,ii}
 T. Junkermann^{63a} A. Juste Rozas^{13,bb} M. K. Juzek⁸⁷ S. Kabana^{137e} A. Kaczmarek⁸⁷ M. Kado¹¹⁰
 H. Kagan¹¹⁹ M. Kagan¹⁴³ A. Kahn⁴¹ A. Kahn¹²⁸ C. Kahra¹⁰¹ T. Kaji¹⁵³ E. Kajomovitz¹⁵⁰ N. Kakati¹⁶⁹
 I. Kalaitzidou⁵⁴ C. W. Kalderon²⁹ A. Kamenshchikov¹⁵⁵ N. J. Kang¹³⁶ D. Kar^{33g} K. Karava¹²⁶
 M. J. Kareem^{156b} E. Karentzos⁵⁴ I. Karkanas¹⁵² O. Karkout¹¹⁴ S. N. Karpov³⁸ Z. M. Karpova³⁸
 V. Kartvelishvili⁹² A. N. Karyukhin³⁷ E. Kasimi¹⁵² J. Katzy⁴⁸ S. Kaur³⁴ K. Kawade¹⁴⁰ M. P. Kawale¹²⁰
 C. Kawamoto⁸⁸ T. Kawamoto¹³⁵ E. F. Kay³⁶ F. I. Kaya¹⁵⁸ S. Kazakos¹⁰⁷ V. F. Kazanin³⁷ Y. Ke¹⁴⁵
 J. M. Keaveney^{33a} R. Keeler¹⁶⁵ G. V. Kehris⁶¹ J. S. Keller³⁴ A. S. Kelly⁹⁷ J. J. Kempster¹⁴⁶ K. E. Kennedy⁴¹
 P. D. Kennedy¹⁰¹ O. Kepka¹³¹ B. P. Kerridge¹⁶⁷ S. Kersten¹⁷¹ B. P. Kerševan⁹⁴ S. Keshri⁶⁶ L. Keszeghova^{28a}
 S. Ketabchi Haghighat¹⁵⁵ R. A. Khan¹²⁹ M. Khandoga¹²⁷ A. Khanov¹²¹ A. G. Kharlamov³⁷ T. Kharlamova³⁷
 E. E. Khoda¹³⁸ M. Kholodenko³⁷ T. J. Khoo¹⁸ G. Khoraiuli¹⁶⁶ J. Khubua^{149b} Y. A. R. Khwaira⁶⁶
 A. Kilgallon¹²³ D. W. Kim^{47a,47b} Y. K. Kim³⁹ N. Kimura⁹⁷ M. K. Kingston⁵⁵ A. Kirchhoff⁵⁵ C. Kirfel²⁴
 F. Kirfel²⁴ J. Kirk¹³⁴ A. E. Kiryunin¹¹⁰ C. Kitsaki¹⁰ O. Kivernyk²⁴ M. Klassen^{63a} C. Klein³⁴ L. Klein¹⁶⁶
 M. H. Klein¹⁰⁶ M. Klein⁹³ S. B. Klein⁵⁶ U. Klein⁹³ P. Klimek³⁶ A. Klimentov²⁹ T. Klioutchnikova³⁶
 P. Kluit¹¹⁴ S. Kluth¹¹⁰ E. Kneringer⁷⁹ T. M. Knight¹⁵⁵ A. Knue⁴⁹ R. Kobayashi⁸⁸ D. Kobylanskii¹⁶⁹
 S. F. Koch¹²⁶ M. Kocian¹⁴³ P. Kodyš¹³³ D. M. Koeck¹²³ P. T. Koenig²⁴ T. Koffas³⁴ M. Kolb¹³⁵
 I. Koletsou⁴ T. Komarek¹²² K. Köneke⁵⁴ A. X. Y. Kong¹ T. Kono¹¹⁸ N. Konstantinidis⁹⁷ P. Kontaxakis⁵⁶
 B. Konya⁹⁹ R. Kopeliansky⁶⁸ S. Koperny^{86a} K. Korcyl⁸⁷ K. Kordas^{152,jj} G. Koren¹⁵¹ A. Korn⁹⁷ S. Korn⁵⁵
 I. Korolkov¹³ N. Korotkova³⁷ B. Kortman¹¹⁴ O. Kortner¹¹⁰ S. Kortner¹¹⁰ W. H. KostECKa¹¹⁵
 V. V. Kostyukhin¹⁴¹ A. Kotsakechagia¹³⁵ A. Kotwal⁵¹ A. Koulouris³⁶ A. Kourkouveli-Charalampidi^{73a,73b}
 C. Kourkouvelis⁹ E. Kourlitis^{110,cc} O. Kovanda¹⁴⁶ R. Kowalewski¹⁶⁵ W. Kozanecki¹³⁵ A. S. Kozhin³⁷
 V. A. Kramarenko³⁷ G. Kramberger⁹⁴ P. Kramer¹⁰¹ M. W. Krasny¹²⁷ A. Krasznahorkay³⁶ J. W. Kraus¹⁷¹
 J. A. Kremer⁴⁸ T. Kresse⁵⁰ J. Kretschmar⁹³ K. Kreul¹⁸ P. Krieger¹⁵⁵ S. Krishnamurthy¹⁰³ M. Krivos¹³³
 K. Krizka²⁰ K. Kroeninger⁴⁹ H. Kroha¹¹⁰ J. Kroll¹³¹ J. Kroll¹²⁸ K. S. Krowpman¹⁰⁷ U. Kruchonak³⁸
 H. Krüger²⁴ N. Krumnack⁸¹ M. C. Kruse⁵¹ J. A. Krzysiak⁸⁷ O. Kuchinskaia³⁷ S. Kuday^{3a} S. Kuehn³⁶
 R. Kuesters⁵⁴ T. Kuhl⁴⁸ V. Kukhtin³⁸ Y. Kulchitsky^{37,p} S. Kuleshov^{137d,137b} M. Kumar^{33g} N. Kumari⁴⁸
 A. Kupco¹³¹ T. Kupfer⁴⁹ A. Kupich³⁷ O. Kuprash⁵⁴ H. Kurashige⁸⁵ L. L. Kurchaninov^{156a} O. Kurdysh⁶⁶
 Y. A. Kurochkin³⁷ A. Kurova³⁷ M. Kuze¹⁵⁴ A. K. Kvam¹⁰³ J. Kvita¹²² T. Kwan¹⁰⁴ N. G. Kyriacou¹⁰⁶

L. A. O. Laatu^{90b} C. Lacasta¹⁶³ F. Lacava^{75a,75b} H. Lacker¹⁸ D. Lacour¹²⁷ N. N. Lad⁹⁷ E. Ladygin³⁸
 B. Laforge¹²⁷ T. Lagouri^{137e} F. Z. Lahbabi^{35a} S. Lai⁵⁵ I. K. Lakomic^{86a} N. Lalloue⁶⁰ J. E. Lambert^{165,1}
 S. Lammers⁶⁸ W. Lampl⁷ C. Lampoudis^{152,ij} A. N. Lancaster¹¹⁵ E. Lançon²⁹ U. Landgraf⁵⁴
 M. P. J. Landon⁹⁵ V. S. Lang⁵⁴ R. J. Langenberg¹⁰³ O. K. B. Langrekken¹²⁵ A. J. Lankford¹⁶⁰ F. Lanni³⁶
 K. Lantzsch²⁴ A. Lanza^{73a} A. Lapertosa^{57b,57a} J. F. Laporte¹³⁵ T. Lari^{71a} F. Lasagni Manghi^{23b} M. Lassnig³⁶
 V. Latonova¹³¹ A. Laudrain¹⁰¹ A. Laurier¹⁵⁰ S. D. Lawlor¹³⁹ Z. Lawrence¹⁰² M. Lazzaroni^{71a,71b} B. Le¹⁰²
 E. M. Le Boulicaut⁵¹ B. Leban⁹⁴ A. Lebedev⁸¹ M. LeBlanc^{102,kk} F. Ledroit-Guillon⁶⁰ A. C. A. Lee⁹⁷
 S. C. Lee¹⁴⁸ S. Lee^{47a,47b} T. F. Lee⁹³ L. L. Leeuw^{33c} H. P. Lefebvre⁹⁶ M. Lefebvre¹⁶⁵ C. Leggett^{17a}
 G. Lehmann Miotto³⁶ M. Leigh⁵⁶ W. A. Leight¹⁰³ W. Leinonen¹¹³ A. Leisos^{152,ll} M. A. L. Leite^{83c}
 C. E. Leitgeb⁴⁸ R. Leitner¹³³ K. J. C. Leney⁴⁴ T. Lenz²⁴ S. Leone^{74a} C. Leonidopoulos⁵² A. Leopold¹⁴⁴
 C. Leroy¹⁰⁸ R. Les¹⁰⁷ C. G. Lester³² M. Levchenko³⁷ J. Levêque⁴ D. Levin¹⁰⁶ L. J. Levinson¹⁶⁹
 M. P. Lewicki⁸⁷ D. J. Lewis⁴ A. Li⁵ B. Li^{62b} C. Li^{62a} C-Q. Li^{62c} H. Li^{62a} H. Li^{62b} H. Li^{14c} H. Li^{14b}
 H. Li^{62b} J. Li^{62c} K. Li¹³⁸ L. Li^{62c} M. Li^{14a,14e} Q. Y. Li^{62a} S. Li^{14a,14e} S. Li^{62d,62c,mm} T. Li^{5,nn} X. Li¹⁰⁴
 Z. Li¹²⁶ Z. Li¹⁰⁴ Z. Li⁹³ Z. Li^{14a,14e} S. Liang^{14a,14e} Z. Liang^{14a} M. Liberatore^{135,oo} B. Liberti^{76a} K. Lie^{64c}
 J. Lieber Marin^{83b} H. Lien⁶⁸ K. Lin¹⁰⁷ R. E. Lindley⁷ J. H. Lindon² E. Lipeles¹²⁸ A. Lipniacka¹⁶
 A. Lister¹⁶⁴ J. D. Little⁴ B. Liu^{14a} B. X. Liu¹⁴² D. Liu^{62d,62c} J. B. Liu^{62a} J. K. K. Liu³² K. Liu^{62d,62c}
 M. Liu^{62a} M. Y. Liu^{62a} P. Liu^{14a} Q. Liu^{62d,138,62c} X. Liu^{62a} Y. Liu^{14d,14e} Y. L. Liu^{62b} Y. W. Liu^{62a}
 J. Llorente Merino¹⁴² S. L. Lloyd⁹⁵ E. M. Lobodzinska⁴⁸ P. Loch⁷ T. Lohse¹⁸ K. Lohwasser¹³⁹
 E. Loiacono⁴⁸ M. Lokajicek^{131,a} J. D. Lomas²⁰ J. D. Long¹⁶² I. Longarini¹⁶⁰ L. Longo^{70a,70b} R. Longo¹⁶²
 I. Lopez Paz⁶⁷ A. Lopez Solis⁴⁸ J. Lorenz¹⁰⁹ N. Lorenzo Martinez⁴ A. M. Lory¹⁰⁹ G. Löschke Centeno¹⁴⁶
 O. Loseva³⁷ X. Lou^{47a,47b} X. Lou^{14a,14e} A. Lounis⁶⁶ J. Love⁶ P. A. Love⁹² G. Lu^{14a,14e} M. Lu⁸⁰ S. Lu¹²⁸
 Y. J. Lu⁶⁵ H. J. Lubatti¹³⁸ C. Luci^{75a,75b} F. L. Lucio Alves^{14c} A. Lucotte⁶⁰ F. Luehring⁶⁸ I. Luise¹⁴⁵
 O. Lukianchuk⁶⁶ O. Lundberg¹⁴⁴ B. Lund-Jensen¹⁴⁴ N. A. Luongo¹²³ M. S. Lutz¹⁵¹ A. B. Lux²⁵ D. Lynn²⁹
 H. Lyons⁹³ R. Lysak¹³¹ E. Lytken⁹⁹ V. Lyubushkin³⁸ T. Lyubushkina³⁸ M. M. Lyukova¹⁴⁵ H. Ma²⁹ K. Ma^{62a}
 L. L. Ma^{62b} Y. Ma¹²¹ D. M. Mac Donell¹⁶⁵ G. Maccarrone⁵³ J. C. MacDonald¹⁰¹
 P. C. Machado De Abreu Farias^{83b} R. Madar⁴⁰ W. F. Mader⁵⁰ T. Madula⁹⁷ J. Maeda⁸⁵ T. Maeno²⁹
 H. Maguire¹³⁹ V. Maiboroda¹³⁵ A. Maio^{130a,130b,130d} K. Maj^{86a} O. Majersky⁴⁸ S. Majewski¹²³ N. Makovec⁶⁶
 V. Maksimovic¹⁵ B. Malaescu¹²⁷ Pa. Malecki⁸⁷ V. P. Maleev³⁷ F. Malek⁶⁰ M. Mali⁹⁴ D. Malito^{96,pp}
 U. Mallik⁸⁰ S. Maltezos¹⁰ S. Malyukov³⁸ J. Mamuzic¹³ G. Mancini⁵³ G. Manco^{73a,73b} J. P. Mandalia⁹⁵
 I. Mandić⁹⁴ L. Manhaes de Andrade Filho^{83a} I. M. Maniatis¹⁶⁹ J. Manjarres Ramos^{90a,qq} D. C. Mankad¹⁶⁹
 A. Mann¹⁰⁹ B. Mansoulie¹³⁵ S. Manzoni³⁶ X. Mapekula^{33c} A. Marantis^{152,ll} G. Marchiori⁵
 M. Marcisovsky¹³¹ C. Marcon^{71a,71b} M. Marinescu²⁰ M. Marjanovic¹²⁰ E. J. Marshall⁹² Z. Marshall^{17a}
 S. Marti-Garcia¹⁶³ T. A. Martin¹⁶⁷ V. J. Martin⁵² B. Martin dit Latour¹⁶ L. Martinelli^{75a,75b} M. Martinez^{13,bb}
 P. Martinez Agullo¹⁶³ V. I. Martinez Outschoorn¹⁰³ P. Martinez Suarez¹³ S. Martin-Haugh¹³⁴ V. S. Martoiu^{27b}
 A. C. Martyniuk⁹⁷ A. Marzin³⁶ D. Mascione^{78a,78b} L. Masetti¹⁰¹ T. Mashimo¹⁵³ J. Masik¹⁰²
 A. L. Maslennikov³⁷ L. Massa^{23b} P. Massarotti^{72a,72b} P. Mastrandrea^{74a,74b} A. Mastroberardino^{43b,43a}
 T. Masubuchi¹⁵³ T. Mathisen¹⁶¹ J. Matousek¹³³ N. Matsuzawa¹⁵³ J. Maurer^{27b} B. Maček⁹⁴ D. A. Maximov³⁷
 R. Mazini¹⁴⁸ I. Maznas¹⁵² M. Mazza¹⁰⁷ S. M. Mazza¹³⁶ E. Mazzeo^{71a,71b} C. Mc Ginn²⁹ J. P. Mc Gowan¹⁰⁴
 S. P. Mc Kee¹⁰⁶ E. F. McDonald¹⁰⁵ A. E. McDougall¹¹⁴ J. A. Mcfayden¹⁴⁶ R. P. McGovern¹²⁸
 G. Mchedlidze^{149b} R. P. Mckenzie^{33g} T. C. Mclachlan⁴⁸ D. J. McLaughlin⁹⁷ S. J. McMahon¹³⁴
 C. M. Mccartland⁹³ R. A. McPherson^{165,t} S. Mehlhase¹⁰⁹ A. Mehta⁹³ D. Melini¹⁵⁰ B. R. Mellado Garcia^{33g}
 A. H. Melo⁵⁵ F. Meloni⁴⁸ A. M. Mendes Jacques Da Costa¹⁰² H. Y. Meng¹⁵⁵ L. Meng⁹² S. Menke¹¹⁰
 M. Mentink³⁶ E. Meoni^{43b,43a} C. Merlassino¹²⁶ L. Merola^{72a,72b} C. Meroni^{71a,71b} G. Merz¹⁰⁶ O. Meshkov³⁷
 J. Metcalfe⁶ A. S. Mete⁶ C. Meyer⁶⁸ J-P. Meyer¹³⁵ R. P. Middleton¹³⁴ L. Mijović⁵² G. Mikenberg¹⁶⁹
 M. Mikesikova¹³¹ M. Mikuž⁹⁴ H. Mildner¹⁰¹ A. Milic³⁶ C. D. Milke⁴⁴ D. W. Miller³⁹ L. S. Miller³⁴
 A. Milov¹⁶⁹ D. A. Milstead^{47a,47b} T. Min^{14c} A. A. Minaenko³⁷ I. A. Minashvili^{149b} L. Mince⁵⁹ A. I. Mincer¹¹⁷
 B. Mindur^{86a} M. Mineev³⁸ Y. Mino⁸⁸ L. M. Mir¹³ M. Miralles Lopez¹⁶³ M. Mironova^{17a} A. Mishima¹⁵³
 M. C. Missio¹¹³ A. Mitra¹⁶⁷ V. A. Mitsou¹⁶³ Y. Mitsumori¹¹¹ O. Miu¹⁵⁵ P. S. Miyagawa⁹⁵ T. Mkrtychyan^{63a}
 M. Mlinarevic⁹⁷ T. Mlinarevic⁹⁷ M. Mlynarikova³⁶ S. Mobius¹⁹ P. Moder⁴⁸ P. Mogg¹⁰⁹

A. F. Mohammed^{14a,14e} S. Mohapatra⁴¹ G. Mokgatitswane^{33g} L. Moleri¹⁶⁹ B. Mondal¹⁴¹ S. Mondal¹³²
K. Mönig⁴⁸ E. Monnier^{90b} L. Monsonis Romero¹⁶³ J. Montejo Berlingen¹³ M. Montella¹¹⁹ F. Montekali^{77a,77b}
F. Monticelli⁹¹ S. Monzani^{69a,69c} N. Morange⁶⁶ A. L. Moreira De Carvalho^{130a} M. Moreno Llácer¹⁶³
C. Moreno Martinez⁵⁶ P. Moretini^{57b} S. Morgenstern³⁶ M. Morii⁶¹ M. Morinaga¹⁵³ A. K. Morley³⁶
F. Morodei^{75a,75b} L. Morvaj³⁶ P. Moschovakos³⁶ B. Moser³⁶ M. Mosidze^{149b} T. Moskalets⁵⁴ P. Moskvitina¹¹³
J. Moss^{31,rr} E. J. W. Moyses¹⁰³ O. Mtintsilana^{33g} S. Muanza^{90b} J. Mueller¹²⁹ D. Muenstermann⁹² R. Müller¹⁹
G. A. Mullier¹⁶¹ A. J. Mullin³² J. J. Mullin¹²⁸ D. P. Mungo¹⁵⁵ D. Munoz Perez¹⁶³ F. J. Munoz Sanchez¹⁰²
M. Murin¹⁰² W. J. Murray^{167,134} A. Murrone^{71a,71b} M. Muškinja^{17a} C. Mwewa²⁹ A. G. Myagkov^{37,p}
A. J. Myers⁸ G. Myers⁶⁸ M. Myska¹³² B. P. Nachman^{17a} O. Nackenhorst⁴⁹ A. Nag⁵⁰ K. Nagai¹²⁶
K. Nagano⁸⁴ J. L. Nagle^{29j} E. Nagy^{90b} A. M. Nairz³⁶ Y. Nakahama⁸⁴ K. Nakamura⁸⁴ K. Nakkalil⁵
H. Nanjo¹²⁴ R. Narayan⁴⁴ E. A. Narayanan¹¹² I. Naryshkin³⁷ M. Naseri³⁴ S. Nasri¹⁵⁹ C. Nass²⁴
G. Navarro^{22a} J. Navarro-Gonzalez¹⁶³ R. Nayak¹⁵¹ A. Nayaz¹⁸ P. Y. Nechaeva³⁷ F. Nechansky⁴⁸
L. Nedic¹²⁶ T. J. Neep²⁰ A. Negri^{73a,73b} M. Negrini^{23b} C. Nellist¹¹⁴ C. Nelson¹⁰⁴ K. Nelson¹⁰⁶
S. Nemecek¹³¹ M. Nessi^{36,ss} M. S. Neubauer¹⁶² F. Neuhaus¹⁰¹ J. Neundorff⁴⁸ R. Newhouse¹⁶⁴
P. R. Newman²⁰ C. W. Ng¹²⁹ Y. W. Y. Ng⁴⁸ B. Ngair^{35e} H. D. N. Nguyen¹⁰⁸ R. B. Nickerson¹²⁶
R. Nicolaidou¹³⁵ J. Nielsen¹³⁶ M. Niemeyer⁵⁵ J. Niermann^{55,36} N. Nikiforou³⁶ V. Nikolaenko^{37,p}
I. Nikolic-Audit¹²⁷ K. Nikolopoulos²⁰ P. Nilsson²⁹ I. Ninca⁴⁸ H. R. Nindhito⁵⁶ G. Ninio¹⁵¹ A. Nisati^{75a}
N. Nishu² R. Nisius¹¹⁰ J.-E. Nitschke⁵⁰ E. K. Nkadimeng^{33g} T. Nobe¹⁵³ D. L. Noel³² T. Nommensen¹⁴⁷
M. B. Norfolk¹³⁹ R. R. B. Norisam⁹⁷ B. J. Norman³⁴ J. Novak⁹⁴ T. Novak⁴⁸ L. Novotny¹³² R. Novotny¹¹²
L. Nozka¹²² K. Ntekas¹⁶⁰ N. M. J. Nunes De Moura Junior^{83b} E. Nurse⁹⁷ J. Ocariz¹²⁷ A. Ochi⁸⁵ I. Ochoa^{130a}
S. Oerdek^{48,tt} J. T. Offermann³⁹ A. Ogrodnik¹³³ A. Oh¹⁰² C. C. Ohm¹⁴⁴ H. Oide⁸⁴ R. Oishi¹⁵³
M. L. Ojeda⁴⁸ M. W. O’Keefe⁹³ Y. Okumura¹⁵³ L. F. Oleiro Seabra^{130a} S. A. Olivares Pino^{137d}
D. Oliveira Damazio²⁹ D. Oliveira Goncalves^{83a} J. L. Oliver¹⁶⁰ Ö. O. Öncel⁵⁴ A. P. O’Neill¹⁹
A. Onofre^{130a,130e} P. U. E. Onyisi¹¹ M. J. Oreglia³⁹ G. E. Orellana⁹¹ D. Orestano^{77a,77b} N. Orlando¹³
R. S. Orr¹⁵⁵ V. O’Shea⁵⁹ L. M. Osojnak¹²⁸ R. Ospanov^{62a} G. Otero y Garzon³⁰ H. Otono⁸⁹ P. S. Ott^{63a}
G. J. Ottino^{17a} M. Ouchrif^{35d} J. Ouellette²⁹ F. Ould-Saada¹²⁵ M. Owen⁵⁹ R. E. Owen¹³⁴ K. Y. Oyulmaz^{21a}
V. E. Ozcan^{21a} F. Ozturk⁸⁷ N. Ozturk⁸ S. Ozturk⁸² H. A. Pacey¹²⁶ A. Pacheco Pages¹³ C. Padilla Aranda¹³
G. Padovano^{75a,75b} S. Pagan Griso^{17a} G. Palacino⁶⁸ A. Palazzo^{70a,70b} S. Palestini³⁶ J. Pan¹⁷² T. Pan^{64a}
D. K. Panchal¹¹ C. E. Pandini¹¹⁴ J. G. Panduro Vazquez⁹⁶ H. D. Pandya¹ H. Pang^{14b} P. Pani⁴⁸
G. Panizzo^{69a,69c} L. Paolozzi⁵⁶ C. Papadatos¹⁰⁸ S. Parajuli⁴⁴ A. Paramonov⁶ C. Paraskevopoulos¹⁰
D. Paredes Hernandez^{64b} K. R. Park⁴¹ T. H. Park¹⁵⁵ M. A. Parker³² F. Parodi^{57b,57a} E. W. Parrish¹¹⁵
V. A. Parrish⁵² J. A. Parsons⁴¹ U. Parzefall⁵⁴ B. Pascual Dias¹⁰⁸ L. Pascual Dominguez¹⁵¹ E. Pasqualucci^{75a}
S. Passaggio^{57b} F. Pastore⁹⁶ P. Pasuwan^{47a,47b} P. Patel⁸⁷ U. M. Patel⁵¹ J. R. Pater¹⁰² T. Pauly³⁶
J. Parkes¹⁴³ M. Pedersen¹²⁵ R. Pedro^{130a} S. V. Peleganchuk³⁷ O. Penc³⁶ E. A. Pender⁵² K. E. Pensi¹⁰⁹
M. Penzin³⁷ B. S. Peralva^{83d} A. P. Pereira Peixoto⁶⁰ L. Pereira Sanchez^{47a,47b} D. V. Perepelitsa^{29j}
E. Perez Codina^{156a} M. Perganti¹⁰ L. Perini^{71a,71b,a} H. Pernegger³⁶ O. Perrin⁴⁰ K. Peters⁴⁸ R. F. Y. Peters¹⁰²
B. A. Petersen³⁶ T. C. Petersen⁴² E. Petit^{90b} V. Petousis¹³² C. Petridou^{152,jj} A. Petrukhin¹⁴¹ M. Pettee^{17a}
N. E. Pettersson³⁶ A. Petukhov³⁷ K. Petukhova¹³³ R. Pezoa^{137f} L. Pezzotti³⁶ G. Pezzullo¹⁷² T. M. Pham¹⁷⁰
T. Pham¹⁰⁵ P. W. Phillips¹³⁴ G. Piacquadio¹⁴⁵ E. Pianori^{17a} F. Piazza¹²³ R. Piegaia³⁰ D. Pietreanu^{27b}
A. D. Pilkington¹⁰² M. Pinamonti^{69a,69c} J. L. Pinfold² B. C. Pinheiro Pereira^{130a} A. E. Pinto Pinoargote^{101,135}
L. Pintucci^{69a,69c} K. M. Piper¹⁴⁶ A. Pirttikoski⁵⁶ D. A. Pizzi³⁴ L. Pizzimento^{64b} A. Pizzini¹¹⁴ M.-A. Pleier²⁹
V. Plesanovs⁵⁴ V. Pleskot¹³³ E. Plotnikova³⁸ G. Poddar⁴ R. Poettgen⁹⁹ L. Poggioli¹²⁷ I. Pokharel⁵⁵
S. Polacek¹³³ G. Polesello^{73a} A. Poley^{142,156a} R. Polifka¹³² A. Polini^{23b} C. S. Pollard¹⁶⁷ Z. B. Pollock¹¹⁹
V. Polychronakos²⁹ E. Pompa Pacchi^{75a,75b} D. Ponomarenko¹¹³ L. Pontecorvo³⁶ S. Popa^{27a}
G. A. Popeneciu^{27d} A. Poreba³⁶ D. M. Portillo Quintero^{156a} S. Pospisil¹³² M. A. Postill¹³⁹ P. Postolache^{27c}
K. Potamianos¹⁶⁷ P. A. Potepa^{86a} I. N. Potrap³⁸ C. J. Potter³² H. Potti¹ T. Poulsen⁴⁸ J. Poveda¹⁶³
M. E. Pozo Astigarraga³⁶ A. Prades Ibanez¹⁶³ J. Pretel⁵⁴ D. Price¹⁰² M. Primavera^{70a} M. A. Principe Martin¹⁰⁰
R. Privara¹²² T. Procter⁵⁹ M. L. Proffitt¹³⁸ N. Proklova¹²⁸ K. Prokofiev^{64c} G. Proto¹¹⁰ S. Protopopescu²⁹
J. Proudfoot⁶ M. Przybycien^{86a} W. W. Przygoda^{86b} J. E. Puddefoot¹³⁹ D. Pudzha³⁷ D. Pyatiizbyantseva³⁷

- J. Qian¹⁰⁶ D. Qichen¹⁰² Y. Qin¹⁰² T. Qiu⁵² A. Quadt⁵⁵ M. Queitsch-Maitland¹⁰² G. Quetant⁵⁶
R. P. Quinn¹⁶⁴ G. Rabanal Bolanos⁶¹ D. Rafanoharana⁵⁴ F. Ragusa^{71a,71b} J. L. Rainbolt³⁹ J. A. Raine⁵⁶
S. Rajagopalan²⁹ E. Ramakoti³⁷ K. Ran^{48,14e} N. P. Rapheeha^{33g} H. Rasheed^{27b} V. Raskina¹²⁷
D. F. Rassloff^{63a} S. Rave¹⁰¹ B. Ravina⁵⁵ I. Ravinovich¹⁶⁹ M. Raymond³⁶ A. L. Read¹²⁵ N. P. Readioff¹³⁹
D. M. Rebuzzi^{73a,73b} G. Redlinger²⁹ A. S. Reed¹¹⁰ K. Reeves²⁶ J. A. Reidelsturz^{171,uu} D. Reikher¹⁵¹
A. Rej^{49,vv} C. Rembser³⁶ A. Renardi⁴⁸ M. Renda^{27b} M. B. Rendel¹¹⁰ F. Renner⁴⁸ A. G. Rennie¹⁶⁰
A. L. Rescia⁴⁸ S. Resconi^{71a} M. Ressegotti^{57b,57a} S. Rettie³⁶ J. G. Reyes Rivera¹⁰⁷ E. Reynolds^{17a}
O. L. Rezanova³⁷ P. Reznicek¹³³ N. Ribaric⁹² E. Ricci^{78a,78b} R. Richter¹¹⁰ S. Richter^{47a,47b}
E. Richter-Was^{86b} M. Ridel¹²⁷ S. Ridouani^{35d} P. Rieck¹¹⁷ P. Riedler³⁶ E. M. Riefel^{47a,47b} J. O. Rieger¹¹⁴
M. Rijssenbeek¹⁴⁵ A. Rimoldi^{73a,73b} M. Rimoldi³⁶ L. Rinaldi^{23b,23a} T. T. Rinn²⁹ M. P. Rinnagel¹⁰⁹
G. Ripellino¹⁶¹ I. Riu¹³ P. Rivadeneira⁴⁸ J. C. Rivera Vergara¹⁶⁵ F. Rizatdinova¹²¹ E. Rizvi⁹⁵
B. A. Roberts¹⁶⁷ B. R. Roberts^{17a} S. H. Robertson^{104,t} D. Robinson³² C. M. Robles Gajardo^{137f}
M. Robles Manzano¹⁰¹ A. Robson⁵⁹ A. Rocchi^{76a,76b} C. Roda^{74a,74b} S. Rodriguez Bosca^{63a}
Y. Rodriguez Garcia^{22a} A. Rodriguez Rodriguez⁵⁴ A. M. Rodríguez Vera^{156b} S. Roe³⁶ J. T. Roemer¹⁶⁰
A. R. Roepe-Gier¹³⁶ J. Roggel¹⁷¹ O. Røhne¹²⁵ R. A. Rojas¹⁰³ C. P. A. Roland¹²⁷ J. Roloff²⁹
A. Romaniouk³⁷ E. Romano^{73a,73b} M. Romano^{23b} A. C. Romero Hernandez¹⁶² N. Rompotis⁹³ L. Roos¹²⁷
S. Rosati^{75a} B. J. Rosser³⁹ E. Rossi¹²⁶ E. Rossi^{72a,72b} L. P. Rossi^{57b} L. Rossini⁵⁴ R. Rosten¹¹⁹
M. Rotaru^{27b} B. Rottler⁵⁴ C. Rougier^{90a,qq} D. Rousseau⁶⁶ D. Rouso³² A. Roy¹⁶² S. Roy-Garand¹⁵⁵
A. Rozanov^{90b} Y. Rozen¹⁵⁰ X. Ruan^{33g} A. Rubio Jimenez¹⁶³ A. J. Ruby⁹³ V. H. Ruelas Rivera¹⁸
T. A. Ruggeri¹ A. Ruggiero¹²⁶ A. Ruiz-Martinez¹⁶³ A. Rummler³⁶ Z. Rurikova⁵⁴ N. A. Rusakovich³⁸
H. L. Russell¹⁶⁵ G. Russo^{75a,75b} J. P. Rutherford⁷ S. Rutherford Colmenares³² K. Rybacki⁹² M. Rybar¹³³
E. B. Rye¹²⁵ A. Ryzhov⁴⁴ J. A. Sabater Iglesias⁵⁶ P. Sabatini¹⁶³ L. Sabetta^{75a,75b} H. F-W. Sadrozinski¹³⁶
F. Safai Tehrani^{75a} B. Safarzadeh Samani¹³⁴ M. Safdari¹⁴³ S. Saha¹⁶⁵ M. Sahinsoy¹¹⁰ M. Saimpert¹³⁵
M. Saito¹⁵³ T. Saito¹⁵³ D. Salamani³⁶ A. Salnikov¹⁴³ J. Salt¹⁶³ A. Salvador Salas¹⁵¹ D. Salvatore^{43b,43a}
F. Salvatore¹⁴⁶ A. Salzburger³⁶ D. Sammel⁵⁴ D. Sampsonidis^{152,jj} D. Sampsonidou¹²³ J. Sánchez¹⁶³
A. Sanchez Pineda⁴ V. Sanchez Sebastian¹⁶³ H. Sandaker¹²⁵ C. O. Sander⁴⁸ J. A. Sandesara¹⁰³ M. Sandhoff¹⁷¹
C. Sandoval^{22b} D. P. C. Sankey¹³⁴ T. Sano⁸⁸ A. Sansoni⁵³ L. Santi^{75a,75b} C. Santoni⁴⁰ H. Santos^{130a,130b}
S. N. Santpur^{17a} A. Santra¹⁶⁹ K. A. Saoucha^{116b} J. G. Saraiva^{130a,130d} J. Sardain⁷ O. Sasaki⁸⁴ K. Sato¹⁵⁷
C. Sauer^{63b} F. Sauerburger⁵⁴ E. Sauvan⁴ P. Savard^{155,e} R. Sawada¹⁵³ C. Sawyer¹³⁴ L. Sawyer⁹⁸
I. Sayago Galvan¹⁶³ C. Sbarra^{23b} A. Sbrizzi^{23b,23a} T. Scanlon⁹⁷ J. Schaarschmidt¹³⁸ P. Schacht¹¹⁰
U. Schäfer¹⁰¹ A. C. Schaffer^{66,44} D. Schaile¹⁰⁹ R. D. Schamberger¹⁴⁵ C. Scharf¹⁸ M. M. Schefer¹⁹
V. A. Schegelsky³⁷ D. Scheirich¹³³ F. Schenck¹⁸ M. Schernau¹⁶⁰ C. Scheulen⁵⁵ C. Schiavi^{57b,57a}
E. J. Schioppa^{70a,70b} M. Schioppa^{43b,43a} B. Schlag^{143,z} K. E. Schleicher⁵⁴ S. Schlenker³⁶ J. Schmeing¹⁷¹
M. A. Schmidt¹⁷¹ K. Schmieden¹⁰¹ C. Schmitt¹⁰¹ N. Schmitt¹⁰¹ S. Schmitt⁴⁸ L. Schoeffel¹³⁵
A. Schoening^{63b} P. G. Scholer⁵⁴ E. Schopf¹²⁶ M. Schott¹⁰¹ J. Schovancova³⁶ S. Schramm⁵⁶ F. Schroeder¹⁷¹
T. Schroer⁵⁶ H-C. Schultz-Coulon^{63a} M. Schumacher⁵⁴ B. A. Schumm¹³⁶ Ph. Schune¹³⁵ A. J. Schuy¹³⁸
H. R. Schwartz¹³⁶ A. Schwartzman¹⁴³ T. A. Schwarz¹⁰⁶ Ph. Schwemling¹³⁵ R. Schvienhorst¹⁰⁷
A. Sciandra¹³⁶ G. Sciolla²⁶ F. Scuri^{74a} C. D. Sebastiani⁹³ K. Sedlaczek¹¹⁵ P. Seema¹⁸ S. C. Seidel¹¹²
A. Seiden¹³⁶ B. D. Seidlitz⁴¹ C. Seitz⁴⁸ J. M. Seixas^{83b} G. Sekhniaidze^{72a} S. J. Sekula⁴⁴ L. Selem⁶⁰
N. Semprini-Cesari^{23b,23a} D. Sengupta⁵⁶ V. Senthilkumar¹⁶³ L. Serin⁶⁶ L. Serkin^{69a,69b} M. Sessa^{76a,76b}
H. Severini¹²⁰ F. Sforza^{57b,57a} A. Sfyrla⁵⁶ E. Shabalina⁵⁵ R. Shaheen¹⁴⁴ J. D. Shahinian¹²⁸
D. Shaked Renous¹⁶⁹ L. Y. Shan^{14a} M. Shapiro^{17a} A. Sharma³⁶ A. S. Sharma¹⁶⁴ P. Sharma⁸⁰ S. Sharma⁴⁸
P. B. Shatalov³⁷ K. Shaw¹⁴⁶ S. M. Shaw¹⁰² A. Shcherbakova³⁷ Q. Shen^{62c,5} P. Sherwood⁹⁷ L. Shi⁹⁷
X. Shi^{14a} C. O. Shimmin¹⁷² J. D. Shinner⁹⁶ I. P. J. Shipsey¹²⁶ S. Shirabe^{56,ss} M. Shiyakova^{38,ww} J. Shlomi¹⁶⁹
M. J. Shochet³⁹ J. Shojaii¹⁰⁵ D. R. Shope¹²⁵ B. Shrestha¹²⁰ S. Shrestha^{119,xx} E. M. Shrif^{33g} M. J. Shroff¹⁶⁵
P. Sicho¹³¹ A. M. Sickles¹⁶² E. Sideras Haddad^{33g} A. Sidoti^{23b} F. Siegert⁵⁰ Dj. Sijacki¹⁵ R. Sikora^{86a}
F. Sili⁹¹ J. M. Silva²⁰ M. V. Silva Oliveira²⁹ S. B. Silverstein^{47a} S. Simion⁶⁶ R. Simoniello³⁶ E. L. Simpson⁵⁹
H. Simpson¹⁴⁶ L. R. Simpson¹⁰⁶ N. D. Simpson⁹⁹ S. Simsek⁸² S. Sindhu⁵⁵ P. Sinervo¹⁵⁵ S. Singh¹⁵⁵
S. Sinha⁴⁸ S. Sinha¹⁰² M. Sioli^{23b,23a} I. Siral³⁶ E. Sitnikova⁴⁸ S. Yu. Sivoklovov^{37,a} J. Sjölin^{47a,47b}

A. Skaf⁵⁵ E. Skorda^{20,yy} P. Skubic¹²⁰ M. Slawinska⁸⁷ V. Smakhtin¹⁶⁹ B. H. Smart¹³⁴ J. Smiesko³⁶
 S. Yu. Smirnov³⁷ Y. Smirnov³⁷ L. N. Smirnova^{37,p} O. Smirnova⁹⁹ A. C. Smith⁴¹ E. A. Smith³⁹
 H. A. Smith¹²⁶ J. L. Smith⁹³ R. Smith¹⁴³ M. Smizanska⁹² K. Smolek¹³² A. A. Snesarev³⁷ S. R. Snider¹⁵⁵
 H. L. Snoek¹¹⁴ S. Snyder²⁹ R. Sobie^{165,t} A. Soffer¹⁵¹ C. A. Solans Sanchez³⁶ E. Yu. Soldatov³⁷
 U. Soldevila¹⁶³ A. A. Solodkov³⁷ S. Solomon²⁶ A. Soloshenko³⁸ K. Solovieva⁵⁴ O. V. Solovyanov⁴⁰
 V. Solovye³⁷ P. Sommer³⁶ A. Sonay¹³ W. Y. Song^{156b} J. M. Sonneveld¹¹⁴ A. Sopczak¹³² A. L. Sopio⁹⁷
 F. Sopkova^{28b} I. R. Sotarriva Alvarez¹⁵⁴ V. Sothilingam^{63a} S. Sottocornola⁶⁸ R. Soualah^{116b} Z. Soumami^{35e}
 D. South⁴⁸ N. Soybelman¹⁶⁹ S. Spagnolo^{70a,70b} M. Spalla¹¹⁰ D. Sperlich⁵⁴ G. Spigo³⁶ S. Spinali⁹²
 D. P. Spiteri⁵⁹ M. Spousta¹³³ E. J. Staats³⁴ A. Stabile^{71a,71b} R. Stamen^{63a} A. Stampekis²⁰ M. Standke²⁴
 E. Stanecka⁸⁷ M. V. Stange⁵⁰ B. Stanislaus^{17a} M. M. Stanitzki⁴⁸ B. Stapf⁴⁸ E. A. Starchenko³⁷
 G. H. Stark¹³⁶ J. Stark^{90a,qq} D. M. Starko^{156b} P. Staroba¹³¹ P. Starovoitov^{63a} S. Stärz¹⁰⁴ R. Staszewski⁸⁷
 G. Stavropoulos⁴⁶ J. Steentoft¹⁶¹ P. Steinberg²⁹ B. Stelzer^{142,156a} H. J. Stelzer¹²⁹ O. Stelzer-Chilton^{156a}
 H. Stenzel⁵⁸ T. J. Stevenson¹⁴⁶ G. A. Stewart³⁶ J. R. Stewart¹²¹ M. C. Stockton³⁶ G. Stoicea^{27b}
 M. Stolarski^{130a} S. Stonjek¹¹⁰ A. Straessner⁵⁰ J. Strandberg¹⁴⁴ S. Strandberg^{47a,47b} M. Stratmann¹⁷¹
 M. Strauss¹²⁰ T. Strebler^{90b} P. Strizenec^{28b} R. Ströhmer¹⁶⁶ D. M. Strom¹²³ L. R. Strom⁴⁸ R. Stroynowski⁴⁴
 A. Strubig^{47a,47b} S. A. Stucci²⁹ B. Stugu¹⁶ J. Stupak¹²⁰ N. A. Styles⁴⁸ D. Su¹⁴³ S. Su^{62a} W. Su^{62d}
 X. Su^{62a,66} K. Sugizaki¹⁵³ V. V. Sulini³⁷ M. J. Sullivan⁹³ D. M. S. Sultan^{78a,78b} L. Sultanaliyeva³⁷
 S. Sultansoy^{3b} T. Sumida⁸⁸ S. Sun¹⁰⁶ S. Sun¹⁷⁰ O. Sunneborn Gudnadottir¹⁶¹ N. Sur^{90b} M. R. Sutton¹⁴⁶
 H. Suzuki¹⁵⁷ M. Svatos¹³¹ M. Swiatlowski^{156a} T. Swirski¹⁶⁶ I. Sykora^{28a} M. Sykora¹³³ T. Sykora¹³³
 D. Ta¹⁰¹ K. Tackmann^{48,zz} A. Taffard¹⁶⁰ R. Tafirout^{156a} J. S. Tafoya Vargas⁶⁶ E. P. Takeva⁵² Y. Takubo⁸⁴
 M. Talby^{90b} A. A. Talyshev³⁷ K. C. Tam^{64b} N. M. Tamir¹⁵¹ A. Tanaka¹⁵³ J. Tanaka¹⁵³ R. Tanaka⁶⁶
 M. Tanasini^{57b,57a} Z. Tao¹⁶⁴ S. Tapia Araya^{137f} S. Tapprogge¹⁰¹ A. Tarek Abouelfadl Mohamed¹⁰⁷ S. Tarem¹⁵⁰
 K. Tariq^{14a} G. Tarna^{90b,27b} G. F. Tartarelli^{71a} P. Tas¹³³ M. Tasevsky¹³¹ E. Tassi^{43b,43a} A. C. Tate¹⁶²
 G. Tateno¹⁵³ Y. Tayalati^{35e,aaa} G. N. Taylor¹⁰⁵ W. Taylor^{156b} A. S. Tee¹⁷⁰ R. Teixeira De Lima¹⁴³
 P. Teixeira-Dias⁹⁶ J. J. Teoh¹⁵⁵ K. Terashi¹⁵³ J. Terron¹⁰⁰ S. Terzo¹³ M. Testa⁵³ R. J. Teuscher^{155,t}
 A. Thaler⁷⁹ O. Theiner⁵⁶ N. Themistokleous⁵² T. Theveneaux-Pelzer^{90b} O. Thielmann¹⁷¹ D. W. Thomas⁹⁶
 J. P. Thomas²⁰ E. A. Thompson^{17a} P. D. Thompson²⁰ E. Thomson¹²⁸ Y. Tian⁵⁵ V. Tikhomirov^{37,p}
 Yu. A. Tikhonov³⁷ S. Timoshenko³⁷ D. Timoshyn¹³³ E. X. L. Ting¹ P. Tipton¹⁷² S. H. Tlou^{33g} A. Tnourji⁴⁰
 K. Todome¹⁵⁴ S. Todorova-Nova¹³³ S. Todt⁵⁰ M. Togawa⁸⁴ J. Tojo⁸⁹ S. Tokár^{28a} K. Tokushuku⁸⁴
 O. Toldaiev⁶⁸ R. Tombs³² M. Tomoto^{84,111} L. Tompkins^{143,z} K. W. Topolnicki^{86b} E. Torrence¹²³
 H. Torres^{90a,qq} E. Torró Pastor¹⁶³ M. Toscani³⁰ C. Toscirri³⁹ M. Tost¹¹ D. R. Tovey¹³⁹ A. Traet¹⁶
 I. S. Trandafir^{27b} T. Trefzger¹⁶⁶ A. Tricoli²⁹ I. M. Trigger^{156a} S. Trincaz-Duvoid¹²⁷ D. A. Trischuk²⁶
 B. Trocme⁶⁰ C. Troncon^{71a} L. Truong^{33c} M. Trzebinski⁸⁷ A. Trzupek⁸⁷ F. Tsai¹⁴⁵ M. Tsai¹⁰⁶
 A. Tsiamis^{152,jj} P. V. Tsiarshka³⁷ S. Tsigaridas^{156a} A. Tsirigotis^{152,ll} V. Tsiskaridze¹⁵⁵ E. G. Tskhadadze^{149a}
 M. Tsopoulou^{152,jj} Y. Tsujikawa⁸⁸ I. I. Tsukerman³⁷ V. Tsulaia^{17a} S. Tsuno⁸⁴ O. Tsur¹⁵⁰ K. Tsurii¹¹⁸
 D. Tsybychev¹⁴⁵ Y. Tu^{64b} A. Tudorache^{27b} V. Tudorache^{27b} A. N. Tuna³⁶ S. Turchikhin^{57b,57a}
 I. Turk Cakir^{3a} R. Turra^{71a} T. Turtuvshin^{38,bbb} P. M. Tuts⁴¹ S. Tzamaris^{152,jj} P. Tzani¹⁰ E. Tzovara¹⁰¹
 F. Ukegawa¹⁵⁷ P. A. Ulloa Poblete^{137c,137b} E. N. Umaka²⁹ G. Unal³⁶ M. Unal¹¹ A. Undrus²⁹ G. Unel¹⁶⁰
 J. Urban^{28b} P. Urquijo¹⁰⁵ P. Urrejola^{137a} G. Usai⁸ R. Ushioda¹⁵⁴ M. Usman¹⁰⁸ Z. Uysal^{21b} V. Vacek¹³²
 B. Vachon¹⁰⁴ K. O. H. Vadla¹²⁵ T. Vafeiadis³⁶ A. Vaitkus⁹⁷ C. Valderanis¹⁰⁹ E. Valdes Santurio^{47a,47b}
 M. Valente^{156a} S. Valentinetti^{23b,23a} A. Valero¹⁶³ E. Valiente Moreno¹⁶³ A. Vallier^{90a,qq} J. A. Valls Ferrer¹⁶³
 D. R. Van Arneman¹¹⁴ T. R. Van Daalen¹³⁸ A. Van Der Graaf⁴⁹ P. Van Gemmeren⁶ M. Van Rijnbach^{125,36}
 S. Van Stroud⁹⁷ I. Van Vulpen¹¹⁴ M. Vanadia^{76a,76b} W. Vandelli³⁶ M. Vandenbroucke¹³⁵ E. R. Vandewall¹²¹
 D. Vannicola¹⁵¹ L. Vannoli^{57b,57a} R. Vari^{75a} E. W. Varnes⁷ C. Varni^{17b} T. Varol¹⁴⁸ D. Varouchas⁶⁶
 L. Varriale¹⁶³ K. E. Varvell¹⁴⁷ M. E. Vasile^{27b} L. Vaslin⁸⁴ G. A. Vasquez¹⁶⁵ A. Vasyukov³⁸ F. Vazeille⁴⁰
 T. Vazquez Schroeder³⁶ J. Veatch³¹ V. Vecchio¹⁰² M. J. Veen¹⁰³ I. Veliscek¹²⁶ L. M. Veloce¹⁵⁵
 F. Veloso^{130a,130c} S. Veneziano^{75a} A. Ventura^{70a,70b} S. Ventura Gonzalez¹³⁵ A. Verbytskyi¹¹⁰ M. Verducci^{74a,74b}
 C. Vergis²⁴ M. Verissimo De Araujo^{83b} W. Verkerke¹¹⁴ J. C. Vermeulen¹¹⁴ C. Vernieri¹⁴³ M. Vessella¹⁰³
 M. C. Vetterli^{142,e} A. Vgenopoulos^{152,jj} N. Viaux Maira^{137f} T. Vickey¹³⁹ O. E. Vickey Boeriu¹³⁹

G. H. A. Viehhauser¹²⁶ L. Vigani^{63b} M. Villa^{23b,23a} M. Villaplana Perez¹⁶³ E. M. Villhauer⁵² E. Vilucchi⁵³
M. G. Vinciter³⁴ G. S. Virdee²⁰ A. Vishwakarma⁵² A. Visibile¹¹⁴ C. Vittori³⁶ I. Vivarelli¹⁴⁶ E. Voevodina¹¹⁰
F. Vogel¹⁰⁹ J. C. Voigt⁵⁰ P. Vokac¹³² Yu. Volkotrub^{86a} J. Von Ahnen⁴⁸ E. Von Toerne²⁴ B. Vormwald³⁶
V. Vorobel¹³³ K. Vorobev³⁷ M. Vos¹⁶³ K. Voss¹⁴¹ J. H. Vosseveld⁹³ M. Vozak¹¹⁴ L. Vozdecky⁹⁵
N. Vranjes¹⁵ M. Vranjes Milosavljevic¹⁵ M. Vreeswijk¹¹⁴ R. Vuillemet³⁶ O. Vujanovic¹⁰¹ I. Vukotic³⁹
S. Wada¹⁵⁷ C. Wagner¹⁰³ J. M. Wagner^{17a} W. Wagner¹⁷¹ S. Wahdan¹⁷¹ H. Wahlberg⁹¹ M. Wakida¹¹¹
J. Walder¹³⁴ R. Walker¹⁰⁹ W. Walkowiak¹⁴¹ A. Wall¹²⁸ T. Wamorkar⁶ A. Z. Wang¹³⁶ C. Wang¹⁰¹
C. Wang^{62c} H. Wang^{17a} J. Wang^{64a} R.-J. Wang¹⁰¹ R. Wang⁶¹ R. Wang⁶ S. M. Wang¹⁴⁸ S. Wang^{62b}
T. Wang^{62a} W. T. Wang⁸⁰ W. Wang^{14a} X. Wang^{14c} X. Wang¹⁶² X. Wang^{62c} Y. Wang^{62d} Y. Wang^{14c}
Z. Wang¹⁰⁶ Z. Wang^{62d,51,62c} Z. Wang¹⁰⁶ A. Warburton¹⁰⁴ R. J. Ward²⁰ N. Warrack⁵⁹ A. T. Watson²⁰
H. Watson⁵⁹ M. F. Watson²⁰ E. Watton^{59,134} G. Watts¹³⁸ B. M. Waugh⁹⁷ C. Weber²⁹ H. A. Weber¹⁸
M. S. Weber¹⁹ S. M. Weber^{63a} C. Wei^{62a} Y. Wei¹²⁶ A. R. Weidberg¹²⁶ E. J. Weik¹¹⁷ J. Weingarten⁴⁹
M. Weirich¹⁰¹ C. Weiser⁵⁴ C. J. Wells⁴⁸ T. Wenaus²⁹ B. Wendland⁴⁹ T. Wengler³⁶ N. S. Wenke¹¹⁰
N. Wermes²⁴ M. Wessels^{63a} A. M. Wharton⁹² A. S. White⁶¹ A. White⁸ M. J. White¹ D. Whiteson¹⁶⁰
L. Wickremasinghe¹²⁴ W. Wiedenmann¹⁷⁰ C. Wiel⁵⁰ M. Wielers¹³⁴ C. Wiglesworth⁴² D. J. Wilbern¹²⁰
H. G. Wilkens³⁶ D. M. Williams⁴¹ H. H. Williams¹²⁸ S. Williams³² S. Willocq¹⁰³ B. J. Wilson¹⁰²
P. J. Windischhofer³⁹ F. I. Winkel³⁰ F. Winklmeier¹²³ B. T. Winter⁵⁴ J. K. Winter¹⁰² M. Wittgen¹⁴³
M. Wobisch⁹⁸ Z. Wolffs¹¹⁴ J. Wollrath¹⁶⁰ M. W. Wolter⁸⁷ H. Wolters^{130a,130c} A. F. Wongel⁴⁸
E. L. Woodward⁴¹ S. D. Worm⁴⁸ B. K. Wosiek⁸⁷ K. W. Woźniak⁸⁷ S. Wozniowski⁵⁵ K. Wraight⁵⁹ C. Wu²⁰
J. Wu^{14a,14e} M. Wu^{64a} M. Wu¹¹³ S. L. Wu¹⁷⁰ X. Wu⁵⁶ Y. Wu^{62a} Z. Wu¹³⁵ J. Wuerzinger^{110,cc}
T. R. Wyatt¹⁰² B. M. Wynne⁵² S. Xella⁴² L. Xia^{14c} M. Xia^{14b} J. Xiang^{64c} M. Xie^{62a} X. Xie^{62a}
S. Xin^{14a,14e} A. Xiong¹²³ J. Xiong^{17a} D. Xu^{14a} H. Xu^{62a} L. Xu^{62a} R. Xu¹²⁸ T. Xu¹⁰⁶ Y. Xu^{14b} Z. Xu⁵²
Z. Xu^{14a} Z. Xu^{14c} B. Yabsley¹⁴⁷ S. Yacoub^{33a} Y. Yamaguchi¹⁵⁴ E. Yamashita¹⁵³ H. Yamauchi¹⁵⁷
T. Yamazaki^{17a} Y. Yamazaki⁸⁵ J. Yan^{62c} S. Yan¹²⁶ Z. Yan²⁵ H. J. Yang^{62c,62d} H. T. Yang^{62a} S. Yang^{62a}
T. Yang^{64c} X. Yang³⁶ X. Yang^{14a} Y. Yang⁴⁴ Y. Yang^{62a} Z. Yang^{62a} W.-M. Yao^{17a} Y. C. Yap⁴⁸ H. Ye^{14c}
H. Ye⁵⁵ J. Ye^{14a} S. Ye²⁹ X. Ye^{62a} Y. Yeh⁹⁷ I. Yeletsikh³⁸ B. K. Yeo^{17b} M. R. Yexley⁹⁷ P. Yin⁴¹
K. Yorita¹⁶⁸ S. Younas^{27b} C. J. S. Young³⁶ C. Young¹⁴³ C. Yu^{14a,14e,ccc} Y. Yu^{62a} M. Yuan¹⁰⁶ R. Yuan^{62b}
L. Yue⁹⁷ M. Zaazoua^{62a} B. Zabinski⁸⁷ E. Zaid⁵² T. Zakareishvili^{149b} N. Zakharchuk³⁴ S. Zambito⁵⁶
J. A. Zamora Saa^{137d,137b} J. Zang¹⁵³ D. Zanzi⁵⁴ O. Zaplatilek¹³² C. Zeitnitz¹⁷¹ H. Zeng^{14a} J. C. Zeng¹⁶²
D. T. Zenger Jr.²⁶ O. Zenin³⁷ T. Ženiš^{28a} S. Zenz⁹⁵ S. Zerradi^{35a} D. Zerwas⁶⁶ M. Zhai^{14a,14e} B. Zhang^{14c}
D. F. Zhang¹³⁹ J. Zhang^{62b} J. Zhang⁶ K. Zhang^{14a,14e} L. Zhang^{14c} P. Zhang^{14a,14e} R. Zhang¹⁷⁰ S. Zhang¹⁰⁶
S. Zhang⁴⁴ T. Zhang¹⁵³ X. Zhang^{62c} X. Zhang^{62b} Y. Zhang^{62c,5} Y. Zhang⁹⁷ Y. Zhang^{14c} Z. Zhang^{17a}
Z. Zhang⁶⁶ H. Zhao¹³⁸ P. Zhao⁵¹ T. Zhao^{62b} Y. Zhao¹³⁶ Z. Zhao^{62a} A. Zhemchugov³⁸ J. Zheng^{14c}
K. Zheng¹⁶² X. Zheng^{62a} Z. Zheng¹⁴³ D. Zhong¹⁶² B. Zhou¹⁰⁶ H. Zhou⁷ N. Zhou^{62c} Y. Zhou⁷ C. G. Zhu^{62b}
J. Zhu¹⁰⁶ Y. Zhu^{62c} Y. Zhu^{62a} X. Zhuang^{14a} K. Zhukov³⁷ V. Zhulanov³⁷ N. I. Zimine³⁸ J. Zinsser^{63b}
M. Ziolkowski¹⁴¹ L. Živković¹⁵ A. Zoccoli^{23b,23a} K. Zoch⁶¹ T. G. Zorbass¹³⁹ O. Zormpa⁴⁶
W. Zou⁴¹ and L. Zwalinski³⁶

(ATLAS Collaboration)

¹*Department of Physics, University of Adelaide, Adelaide, Australia*²*Department of Physics, University of Alberta, Edmonton, Alberta, Canada*^{3a}*Department of Physics, Ankara University, Ankara, Türkiye*^{3b}*Division of Physics, TOBB University of Economics and Technology, Ankara, Türkiye*⁴*LAPP, Université Savoie Mont Blanc, CNRS/IN2P3, Annecy, France*⁵*APC, Université Paris Cité, CNRS/IN2P3, Paris, France*⁶*High Energy Physics Division, Argonne National Laboratory, Argonne, Illinois, USA*⁷*Department of Physics, University of Arizona, Tucson, Arizona, USA*⁸*Department of Physics, University of Texas at Arlington, Arlington, Texas, USA*⁹*Physics Department, National and Kapodistrian University of Athens, Athens, Greece*¹⁰*Physics Department, National Technical University of Athens, Zografou, Greece*

- ¹¹*Department of Physics, University of Texas at Austin, Austin, Texas, USA*
- ¹²*Institute of Physics, Azerbaijan Academy of Sciences, Baku, Azerbaijan*
- ¹³*Institut de Física d'Altes Energies (IFAE), Barcelona Institute of Science and Technology, Barcelona, Spain*
- ^{14a}*Institute of High Energy Physics, Chinese Academy of Sciences, Beijing, China*
- ^{14b}*Physics Department, Tsinghua University, Beijing, China*
- ^{14c}*Department of Physics, Nanjing University, Nanjing, China*
- ^{14d}*School of Science, Shenzhen Campus of Sun Yat-sen University, China*
- ^{14e}*University of Chinese Academy of Science (UCAS), Beijing, China*
- ¹⁵*Institute of Physics, University of Belgrade, Belgrade, Serbia*
- ¹⁶*Department for Physics and Technology, University of Bergen, Bergen, Norway*
- ^{17a}*Physics Division, Lawrence Berkeley National Laboratory, Berkeley, California, USA*
- ^{17b}*University of California, Berkeley, California, USA*
- ¹⁸*Institut für Physik, Humboldt Universität zu Berlin, Berlin, Germany*
- ¹⁹*Albert Einstein Center for Fundamental Physics and Laboratory for High Energy Physics, University of Bern, Bern, Switzerland*
- ²⁰*School of Physics and Astronomy, University of Birmingham, Birmingham, United Kingdom*
- ^{21a}*Department of Physics, Bogazici University, Istanbul, Türkiye*
- ^{21b}*Department of Physics Engineering, Gaziantep University, Gaziantep, Türkiye*
- ^{21c}*Department of Physics, Istanbul University, Istanbul, Türkiye*
- ^{22a}*Facultad de Ciencias y Centro de Investigaciones, Universidad Antonio Nariño, Bogotá, Colombia*
- ^{22b}*Departamento de Física, Universidad Nacional de Colombia, Bogotá, Colombia*
- ^{23a}*Dipartimento di Fisica e Astronomia A. Righi, Università di Bologna, Bologna, Italy*
- ^{23b}*INFN Sezione di Bologna, Bologna, Italy*
- ²⁴*Physikalisches Institut, Universität Bonn, Bonn, Germany*
- ²⁵*Department of Physics, Boston University, Boston, Massachusetts, USA*
- ²⁶*Department of Physics, Brandeis University, Waltham, Massachusetts, USA*
- ^{27a}*Transilvania University of Brasov, Brasov, Romania*
- ^{27b}*Horia Hulubei National Institute of Physics and Nuclear Engineering, Bucharest, Romania*
- ^{27c}*Department of Physics, Alexandru Ioan Cuza University of Iasi, Iasi, Romania*
- ^{27d}*National Institute for Research and Development of Isotopic and Molecular Technologies, Physics Department, Cluj-Napoca, Romania*
- ^{27e}*University Politehnica Bucharest, Bucharest, Romania*
- ^{27f}*West University in Timisoara, Timisoara, Romania*
- ^{27g}*Faculty of Physics, University of Bucharest, Bucharest, Romania*
- ^{28a}*Faculty of Mathematics, Physics and Informatics, Comenius University, Bratislava, Slovak Republic*
- ^{28b}*Department of Subnuclear Physics, Institute of Experimental Physics of the Slovak Academy of Sciences, Kosice, Slovak Republic*
- ²⁹*Physics Department, Brookhaven National Laboratory, Upton, New York, USA*
- ³⁰*Universidad de Buenos Aires, Facultad de Ciencias Exactas y Naturales, Departamento de Física, CONICET, Instituto de Física de Buenos Aires (IFIBA), Buenos Aires, Argentina*
- ³¹*California State University, California, USA*
- ³²*Cavendish Laboratory, University of Cambridge, Cambridge, United Kingdom*
- ^{33a}*Department of Physics, University of Cape Town, Cape Town, South Africa*
- ^{33b}*iThemba Labs, Western Cape, South Africa*
- ^{33c}*Department of Mechanical Engineering Science, University of Johannesburg, Johannesburg, South Africa*
- ^{33d}*National Institute of Physics, University of the Philippines Diliman, Quezon City, Philippines*
- ^{33e}*University of South Africa, Department of Physics, Pretoria, South Africa*
- ^{33f}*University of Zululand, KwaDlangezwa, South Africa*
- ^{33g}*School of Physics, University of the Witwatersrand, Johannesburg, South Africa*
- ³⁴*Department of Physics, Carleton University, Ottawa, Ontario, Canada*
- ^{35a}*Faculté des Sciences Ain Chock, Réseau Universitaire de Physique des Hautes Energies—Université Hassan II, Casablanca, Morocco*
- ^{35b}*Faculté des Sciences, Université Ibn-Tofail, Kénitra, Morocco*
- ^{35c}*Faculté des Sciences Semlalia, Université Cadi Ayyad, LPHEA-Marrakech, Morocco*
- ^{35d}*LPMR, Faculté des Sciences, Université Mohamed Premier, Oujda, Morocco*
- ^{35e}*Faculté des sciences, Université Mohammed V, Rabat, Morocco*
- ^{35f}*Institute of Applied Physics, Mohammed VI Polytechnic University, Ben Guerir, Morocco*
- ³⁶*CERN, Geneva, Switzerland*

- ³⁷*Affiliated with an institute covered by a cooperation agreement with CERN*
- ³⁸*Affiliated with an international laboratory covered by a cooperation agreement with CERN*
- ³⁹*Enrico Fermi Institute, University of Chicago, Chicago, Illinois, USA*
- ⁴⁰*LPC, Université Clermont Auvergne, CNRS/IN2P3, Clermont-Ferrand, France*
- ⁴¹*Nevis Laboratory, Columbia University, Irvington, New York, USA*
- ⁴²*Niels Bohr Institute, University of Copenhagen, Copenhagen, Denmark*
- ^{43a}*Dipartimento di Fisica, Università della Calabria, Rende, Italy*
- ^{43b}*INFN Gruppo Collegato di Cosenza, Laboratori Nazionali di Frascati, Italy*
- ⁴⁴*Physics Department, Southern Methodist University, Dallas, Texas, USA*
- ⁴⁵*Physics Department, University of Texas at Dallas, Richardson, Texas, USA*
- ⁴⁶*National Centre for Scientific Research “Demokritos,” Agia Paraskevi, Greece*
- ^{47a}*Department of Physics, Stockholm University, Stockholm, Sweden*
- ^{47b}*Oskar Klein Centre, Stockholm, Sweden*
- ⁴⁸*Deutsches Elektronen-Synchrotron DESY, Hamburg and Zeuthen, Germany*
- ⁴⁹*Fakultät Physik, Technische Universität Dortmund, Dortmund, Germany*
- ⁵⁰*Institut für Kern- und Teilchenphysik, Technische Universität Dresden, Dresden, Germany*
- ⁵¹*Department of Physics, Duke University, Durham, North Carolina, USA*
- ⁵²*SUPA—School of Physics and Astronomy, University of Edinburgh, Edinburgh, United Kingdom*
- ⁵³*INFN e Laboratori Nazionali di Frascati, Frascati, Italy*
- ⁵⁴*Physikalisches Institut, Albert-Ludwigs-Universität Freiburg, Freiburg, Germany*
- ⁵⁵*II. Physikalisches Institut, Georg-August-Universität Göttingen, Göttingen, Germany*
- ⁵⁶*Département de Physique Nucléaire et Corpusculaire, Université de Genève, Genève, Switzerland*
- ^{57a}*Dipartimento di Fisica, Università di Genova, Genova, Italy*
- ^{57b}*INFN Sezione di Genova, Genova, Italy*
- ⁵⁸*II. Physikalisches Institut, Justus-Liebig-Universität Giessen, Giessen, Germany*
- ⁵⁹*SUPA—School of Physics and Astronomy, University of Glasgow, Glasgow, United Kingdom*
- ⁶⁰*LPSC, Université Grenoble Alpes, CNRS/IN2P3, Grenoble INP, Grenoble, France*
- ⁶¹*Laboratory for Particle Physics and Cosmology, Harvard University, Cambridge, Massachusetts, USA*
- ^{62a}*Department of Modern Physics and State Key Laboratory of Particle Detection and Electronics, University of Science and Technology of China, Hefei, China*
- ^{62b}*Institute of Frontier and Interdisciplinary Science and Key Laboratory of Particle Physics and Particle Irradiation (MOE), Shandong University, Qingdao, China*
- ^{62c}*School of Physics and Astronomy, Shanghai Jiao Tong University, Key Laboratory for Particle Astrophysics and Cosmology (MOE), SKLPPC, Shanghai, China*
- ^{62d}*Tsung-Dao Lee Institute, Shanghai, China*
- ^{63a}*Kirchhoff-Institut für Physik, Ruprecht-Karls-Universität Heidelberg, Heidelberg, Germany*
- ^{63b}*Physikalisches Institut, Ruprecht-Karls-Universität Heidelberg, Heidelberg, Germany*
- ^{64a}*Department of Physics, Chinese University of Hong Kong, Shatin, N.T., Hong Kong, China*
- ^{64b}*Department of Physics, University of Hong Kong, Hong Kong, China*
- ^{64c}*Department of Physics and Institute for Advanced Study, Hong Kong University of Science and Technology, Clear Water Bay, Kowloon, Hong Kong, China*
- ⁶⁵*Department of Physics, National Tsing Hua University, Hsinchu, Taiwan*
- ⁶⁶*IJCLab, Université Paris-Saclay, CNRS/IN2P3, 91405, Orsay, France*
- ⁶⁷*Centro Nacional de Microelectrónica (IMB-CNM-CSIC), Barcelona, Spain*
- ⁶⁸*Department of Physics, Indiana University, Bloomington, Indiana, USA*
- ^{69a}*INFN Gruppo Collegato di Udine, Sezione di Trieste, Udine, Italy*
- ^{69b}*ICTP, Trieste, Italy*
- ^{69c}*Dipartimento Politecnico di Ingegneria e Architettura, Università di Udine, Udine, Italy*
- ^{70a}*INFN Sezione di Lecce, Lecce, Italy*
- ^{70b}*Dipartimento di Matematica e Fisica, Università del Salento, Lecce, Italy*
- ^{71a}*INFN Sezione di Milano, Milano, Italy*
- ^{71b}*Dipartimento di Fisica, Università di Milano, Milano, Italy*
- ^{72a}*INFN Sezione di Napoli, Napoli, Italy*
- ^{72b}*Dipartimento di Fisica, Università di Napoli, Napoli, Italy*
- ^{73a}*INFN Sezione di Pavia, Pavia, Italy*
- ^{73b}*Dipartimento di Fisica, Università di Pavia, Pavia, Italy*
- ^{74a}*INFN Sezione di Pisa, Pisa, Italy*
- ^{74b}*Dipartimento di Fisica E. Fermi, Università di Pisa, Pisa, Italy*
- ^{75a}*INFN Sezione di Roma, Roma, Italy*
- ^{75b}*Dipartimento di Fisica, Sapienza Università di Roma, Roma, Italy*

- ^{76a}*INFN Sezione di Roma Tor Vergata, Roma, Italy*
^{76b}*Dipartimento di Fisica, Università di Roma Tor Vergata, Roma, Italy*
^{77a}*INFN Sezione di Roma Tre, Roma, Italy*
^{77b}*Dipartimento di Matematica e Fisica, Università Roma Tre, Roma, Italy*
^{78a}*INFN-TIFPA, Trento, Italy*
^{78b}*Università degli Studi di Trento, Trento, Italy*
⁷⁹*Universität Innsbruck, Department of Astro and Particle Physics, Innsbruck, Austria*
⁸⁰*University of Iowa, Iowa City, Iowa, USA*
⁸¹*Department of Physics and Astronomy, Iowa State University, Ames, Iowa, USA*
⁸²*Istinye University, Sariyer, Istanbul, Türkiye*
^{83a}*Departamento de Engenharia Elétrica, Universidade Federal de Juiz de Fora (UFJF), Juiz de Fora, Brazil*
^{83b}*Universidade Federal do Rio De Janeiro COPPE/EE/IF, Rio de Janeiro, Brazil*
^{83c}*Instituto de Física, Universidade de São Paulo, São Paulo, Brazil*
^{83d}*Rio de Janeiro State University, Rio de Janeiro, Brazil*
⁸⁴*KEK, High Energy Accelerator Research Organization, Tsukuba, Japan*
⁸⁵*Graduate School of Science, Kobe University, Kobe, Japan*
^{86a}*AGH University of Krakow, Faculty of Physics and Applied Computer Science, Krakow, Poland*
^{86b}*Marian Smoluchowski Institute of Physics, Jagiellonian University, Krakow, Poland*
⁸⁷*Institute of Nuclear Physics Polish Academy of Sciences, Krakow, Poland*
⁸⁸*Faculty of Science, Kyoto University, Kyoto, Japan*
⁸⁹*Research Center for Advanced Particle Physics and Department of Physics, Kyushu University, Fukuoka, Japan*
^{90a}*L2IT, Université de Toulouse, CNRS/IN2P3, UPS, Toulouse, France*
^{90b}*CPPM, Aix-Marseille Université, CNRS/IN2P3, Marseille, France*
⁹¹*Instituto de Física La Plata, Universidad Nacional de La Plata and CONICET, La Plata, Argentina*
⁹²*Physics Department, Lancaster University, Lancaster, United Kingdom*
⁹³*Oliver Lodge Laboratory, University of Liverpool, Liverpool, United Kingdom*
⁹⁴*Department of Experimental Particle Physics, Jožef Stefan Institute and Department of Physics, University of Ljubljana, Ljubljana, Slovenia*
⁹⁵*School of Physics and Astronomy, Queen Mary University of London, London, United Kingdom*
⁹⁶*Department of Physics, Royal Holloway University of London, Egham, United Kingdom*
⁹⁷*Department of Physics and Astronomy, University College London, London, United Kingdom*
⁹⁸*Louisiana Tech University, Ruston, Louisiana, USA*
⁹⁹*Fysiska institutionen, Lunds universitet, Lund, Sweden*
¹⁰⁰*Departamento de Física Teórica C-15 and CIAFF, Universidad Autónoma de Madrid, Madrid, Spain*
¹⁰¹*Institut für Physik, Universität Mainz, Mainz, Germany*
¹⁰²*School of Physics and Astronomy, University of Manchester, Manchester, United Kingdom*
¹⁰³*Department of Physics, University of Massachusetts, Amherst, Massachusetts, USA*
¹⁰⁴*Department of Physics, McGill University, Montreal, Quebec, Canada*
¹⁰⁵*School of Physics, University of Melbourne, Victoria, Australia*
¹⁰⁶*Department of Physics, University of Michigan, Ann Arbor, Michigan, USA*
¹⁰⁷*Department of Physics and Astronomy, Michigan State University, East Lansing, Michigan, USA*
¹⁰⁸*Group of Particle Physics, University of Montreal, Montreal, Quebec, Canada*
¹⁰⁹*Fakultät für Physik, Ludwig-Maximilians-Universität München, München, Germany*
¹¹⁰*Max-Planck-Institut für Physik (Werner-Heisenberg-Institut), München, Germany*
¹¹¹*Graduate School of Science and Kobayashi-Maskawa Institute, Nagoya University, Nagoya, Japan*
¹¹²*Department of Physics and Astronomy, University of New Mexico, Albuquerque, New Mexico, USA*
¹¹³*Institute for Mathematics, Astrophysics and Particle Physics, Radboud University/Nikhef, Nijmegen, Netherlands*
¹¹⁴*Nikhef National Institute for Subatomic Physics and University of Amsterdam, Amsterdam, Netherlands*
¹¹⁵*Department of Physics, Northern Illinois University, DeKalb, Illinois, USA*
^{116a}*New York University Abu Dhabi, Abu Dhabi, United Arab Emirates*
^{116b}*University of Sharjah, Sharjah, United Arab Emirates*
¹¹⁷*Department of Physics, New York University, New York, New York, USA*
¹¹⁸*Ochanomizu University, Otsuka, Bunkyo-ku, Tokyo, Japan*
¹¹⁹*Ohio State University, Columbus, Ohio, USA*
¹²⁰*Homer L. Dodge Department of Physics and Astronomy, University of Oklahoma, Norman, Oklahoma, USA*
¹²¹*Department of Physics, Oklahoma State University, Stillwater, Oklahoma, USA*

- ¹²²Palacký University, Joint Laboratory of Optics, Olomouc, Czech Republic
- ¹²³Institute for Fundamental Science, University of Oregon, Eugene, Oregon, USA
- ¹²⁴Graduate School of Science, Osaka University, Osaka, Japan
- ¹²⁵Department of Physics, University of Oslo, Oslo, Norway
- ¹²⁶Department of Physics, Oxford University, Oxford, United Kingdom
- ¹²⁷LPNHE, Sorbonne Université, Université Paris Cité, CNRS/IN2P3, Paris, France
- ¹²⁸Department of Physics, University of Pennsylvania, Philadelphia, Pennsylvania, USA
- ¹²⁹Department of Physics and Astronomy, University of Pittsburgh, Pittsburgh, Pennsylvania, USA
- ^{130a}Laboratório de Instrumentação e Física Experimental de Partículas—LIP, Lisboa, Portugal
- ^{130b}Departamento de Física, Faculdade de Ciências, Universidade de Lisboa, Lisboa, Portugal
- ^{130c}Departamento de Física, Universidade de Coimbra, Coimbra, Portugal
- ^{130d}Centro de Física Nuclear da Universidade de Lisboa, Lisboa, Portugal
- ^{130e}Departamento de Física, Universidade do Minho, Braga, Portugal
- ^{130f}Departamento de Física Teórica y del Cosmos, Universidad de Granada, Granada, Spain
- ^{130g}Departamento de Física, Instituto Superior Técnico, Universidade de Lisboa, Lisboa, Portugal
- ¹³¹Institute of Physics of the Czech Academy of Sciences, Prague, Czech Republic
- ¹³²Czech Technical University in Prague, Prague, Czech Republic
- ¹³³Charles University, Faculty of Mathematics and Physics, Prague, Czech Republic
- ¹³⁴Particle Physics Department, Rutherford Appleton Laboratory, Didcot, United Kingdom
- ¹³⁵IRFU, CEA, Université Paris-Saclay, Gif-sur-Yvette, France
- ¹³⁶Santa Cruz Institute for Particle Physics, University of California Santa Cruz, Santa Cruz, California, USA
- ^{137a}Departamento de Física, Pontificia Universidad Católica de Chile, Santiago, Chile
- ^{137b}Millennium Institute for Subatomic Physics at High Energy Frontier (SAPHIR), Santiago, Chile
- ^{137c}Instituto de Investigación Multidisciplinario en Ciencia y Tecnología, y Departamento de Física, Universidad de La Serena, La Serena, Chile
- ^{137d}Universidad Andres Bello, Department of Physics, Santiago, Chile
- ^{137e}Instituto de Alta Investigación, Universidad de Tarapacá, Arica, Chile
- ^{137f}Departamento de Física, Universidad Técnica Federico Santa María, Valparaíso, Chile
- ¹³⁸Department of Physics, University of Washington, Seattle, Washington, USA
- ¹³⁹Department of Physics and Astronomy, University of Sheffield, Sheffield, United Kingdom
- ¹⁴⁰Department of Physics, Shinshu University, Nagano, Japan
- ¹⁴¹Department Physik, Universität Siegen, Siegen, Germany
- ¹⁴²Department of Physics, Simon Fraser University, Burnaby, British Columbia, Canada
- ¹⁴³SLAC National Accelerator Laboratory, Stanford, California, USA
- ¹⁴⁴Department of Physics, Royal Institute of Technology, Stockholm, Sweden
- ¹⁴⁵Departments of Physics and Astronomy, Stony Brook University, Stony Brook, New York, USA
- ¹⁴⁶Department of Physics and Astronomy, University of Sussex, Brighton, United Kingdom
- ¹⁴⁷School of Physics, University of Sydney, Sydney, Australia
- ¹⁴⁸Institute of Physics, Academia Sinica, Taipei, Taiwan
- ^{149a}E. Andronikashvili Institute of Physics, Iv. Javakhishvili Tbilisi State University, Tbilisi, Georgia
- ^{149b}High Energy Physics Institute, Tbilisi State University, Tbilisi, Georgia
- ^{149c}University of Georgia, Tbilisi, Georgia
- ¹⁵⁰Department of Physics, Technion, Israel Institute of Technology, Haifa, Israel
- ¹⁵¹Raymond and Beverly Sackler School of Physics and Astronomy, Tel Aviv University, Tel Aviv, Israel
- ¹⁵²Department of Physics, Aristotle University of Thessaloniki, Thessaloniki, Greece
- ¹⁵³International Center for Elementary Particle Physics and Department of Physics, University of Tokyo, Tokyo, Japan
- ¹⁵⁴Department of Physics, Tokyo Institute of Technology, Tokyo, Japan
- ¹⁵⁵Department of Physics, University of Toronto, Toronto, Ontario, Canada
- ^{156a}TRIUMF, Vancouver, British Columbia, Canada
- ^{156b}Department of Physics and Astronomy, York University, Toronto, Ontario, Canada
- ¹⁵⁷Division of Physics and Tomonaga Center for the History of the Universe, Faculty of Pure and Applied Sciences, University of Tsukuba, Tsukuba, Japan
- ¹⁵⁸Department of Physics and Astronomy, Tufts University, Medford, Massachusetts, USA
- ¹⁵⁹United Arab Emirates University, Al Ain, United Arab Emirates
- ¹⁶⁰Department of Physics and Astronomy, University of California Irvine, Irvine, California, USA
- ¹⁶¹Department of Physics and Astronomy, University of Uppsala, Uppsala, Sweden
- ¹⁶²Department of Physics, University of Illinois, Urbana, Illinois, USA
- ¹⁶³Instituto de Física Corpuscular (IFIC), Centro Mixto Universidad de Valencia—CSIC, Valencia, Spain

¹⁶⁴*Department of Physics, University of British Columbia, Vancouver, British Columbia, Canada*

¹⁶⁵*Department of Physics and Astronomy, University of Victoria, Victoria, British Columbia, Canada*

¹⁶⁶*Fakultät für Physik und Astronomie, Julius-Maximilians-Universität Würzburg, Würzburg, Germany*

¹⁶⁷*Department of Physics, University of Warwick, Coventry, United Kingdom*

¹⁶⁸*Waseda University, Tokyo, Japan*

¹⁶⁹*Department of Particle Physics and Astrophysics, Weizmann Institute of Science, Rehovot, Israel*

¹⁷⁰*Department of Physics, University of Wisconsin, Madison, Wisconsin, USA*

¹⁷¹*Fakultät für Mathematik und Naturwissenschaften, Fachgruppe Physik,
Bergische Universität Wuppertal, Wuppertal, Germany*

¹⁷²*Department of Physics, Yale University, New Haven, Connecticut, USA*

^aDeceased.

^bAlso at Department of Physics, King's College London, London, United Kingdom.

^cAlso at Institute of Physics, Azerbaijan Academy of Sciences, Baku, Azerbaijan.

^dAlso at Lawrence Livermore National Laboratory, Livermore, California, USA.

^eAlso at TRIUMF, Vancouver, British Columbia, Canada.

^fAlso at Department of Physics, University of Thessaly, Greece.

^gAlso at Institut für Physik, Universität Mainz, Mainz, Germany.

^hAlso at An-Najah National University, Nablus, Palestine.

ⁱAlso at Department of Physics, University of Fribourg, Fribourg, Switzerland.

^jAlso at University of Colorado Boulder, Department of Physics, Colorado, Boulder, USA.

^kAlso at SUPA—School of Physics and Astronomy, University of Glasgow, Glasgow, United Kingdom.

^lAlso at Department of Physics and Astronomy, University of Victoria, Victoria, British Columbia, Canada.

^mAlso at CERN Tier-0, Switzerland.

ⁿAlso at Department of Physics, Westmont College, Santa Barbara, California, USA.

^oAlso at Departament de Física de la Universitat Autònoma de Barcelona, Barcelona, Spain.

^pAlso at Affiliated with an institute covered by a cooperation agreement with CERN.

^qAlso at The Collaborative Innovation Center of Quantum Matter (CICQM), Beijing, China.

^rAlso at Department of Physics, Ben Gurion University of the Negev, Beer Sheva, Israel.

^sAlso at Università di Napoli Parthenope, Napoli, Italy.

^tAlso at Institute of Particle Physics (IPP), Canada.

^uAlso at Group of Particle Physics, University of Montreal, Montreal, Quebec, Canada.

^vAlso at Borough of Manhattan Community College, City University of New York, New York, New York, USA.

^wAlso at National Institute of Physics, University of the Philippines Diliman, Philippines.

^xAlso at Department of Financial and Management Engineering, University of the Aegean, Chios, Greece.

^yAlso at Ochanomizu University, Otsuka, Bunkyo-ku, Tokyo, Japan.

^zAlso at Department of Physics, Stanford University, Stanford, California, USA.

^{aa}Also at Centro Studi e Ricerche Enrico Fermi, Italy.

^{bb}Also at Institutio Catalana de Recerca i Estudis Avancats, ICREA, Barcelona, Spain.

^{cc}Also at Technical University of Munich, Munich, Germany.

^{dd}Also at Department of Physics and Astronomy, University of Sheffield, Sheffield, United Kingdom.

^{ee}Also at Department of Physics, Oxford University, Oxford, United Kingdom.

^{ff}Also at Yeditepe University, Physics Department, Istanbul, Türkiye.

^{gg}Also at Institute of Theoretical Physics, Ilia State University, Tbilisi, Georgia.

^{hh}Also at CERN, Geneva, Switzerland.

ⁱⁱAlso at Department of Physics, University of Massachusetts, Amherst, Massachusetts, USA.

^{jj}Also at Center for Interdisciplinary Research and Innovation (CIRI-AUTH), Thessaloniki, Greece.

^{kk}Also at School of Physics and Astronomy, University of Manchester, Manchester, United Kingdom.

^{ll}Also at Hellenic Open University, Patras, Greece.

^{mm}Also at Center for High Energy Physics, Peking University, China.

ⁿⁿAlso at APC, Université Paris Cité, CNRS/IN2P3, Paris, France.

^{oo}Also at IRFU, CEA, Université Paris-Saclay, Gif-sur-Yvette, France.

^{pp}Also at Department of Physics, Royal Holloway University of London, Egham, United Kingdom.

^{qq}Also at L2IT, Université de Toulouse, CNRS/IN2P3, UPS, Toulouse, France.

^{rr}Also at Department of Physics, California State University, Sacramento, California, USA.

^{ss}Also at Département de Physique Nucléaire et Corpusculaire, Université de Genève, Genève, Switzerland.

^{tt}Also at Deutsches Elektronen-Synchrotron DESY, Hamburg and Zeuthen, Germany.

^{uu}Also at Fakultät für Mathematik und Naturwissenschaften, Fachgruppe Physik, Bergische Universität Wuppertal, Wuppertal, Germany.

^{vv}Also at Fakultät Physik, Technische Universität Dortmund, Dortmund, Germany.

^{ww} Also at Institute for Nuclear Research and Nuclear Energy (INRNE) of the Bulgarian Academy of Sciences, Sofia, Bulgaria.

^{xx} Also at Washington College, Chestertown, Maryland, USA.

^{yy} Also at School of Physics and Astronomy, University of Birmingham, Birmingham, United Kingdom.

^{zz} Also at Institut für Experimentalphysik, Universität Hamburg, Hamburg, Germany.

^{aaa} Also at Institute of Applied Physics, Mohammed VI Polytechnic University, Ben Guerir, Morocco.

^{bbb} Also at Institute of Physics and Technology, Ulaanbaatar, Mongolia.

^{ccc} Also at University of Chinese Academy of Sciences (UCAS), Beijing, China.